AD-A048 025 WEAPONS RESEARCH ESTABLISHMENT SALISBURY (AUSTRALIA) F/G 20/4
IMPROVED INTEGRATION TECHNIQUES FOR FLUID FLOW FINITE ELEMENT F--ETC(U)
APR 77 C A FLETCHER

UNCLASSIFIED WRE-TR-1810(W) NL

1 OF 1
ADA048 025

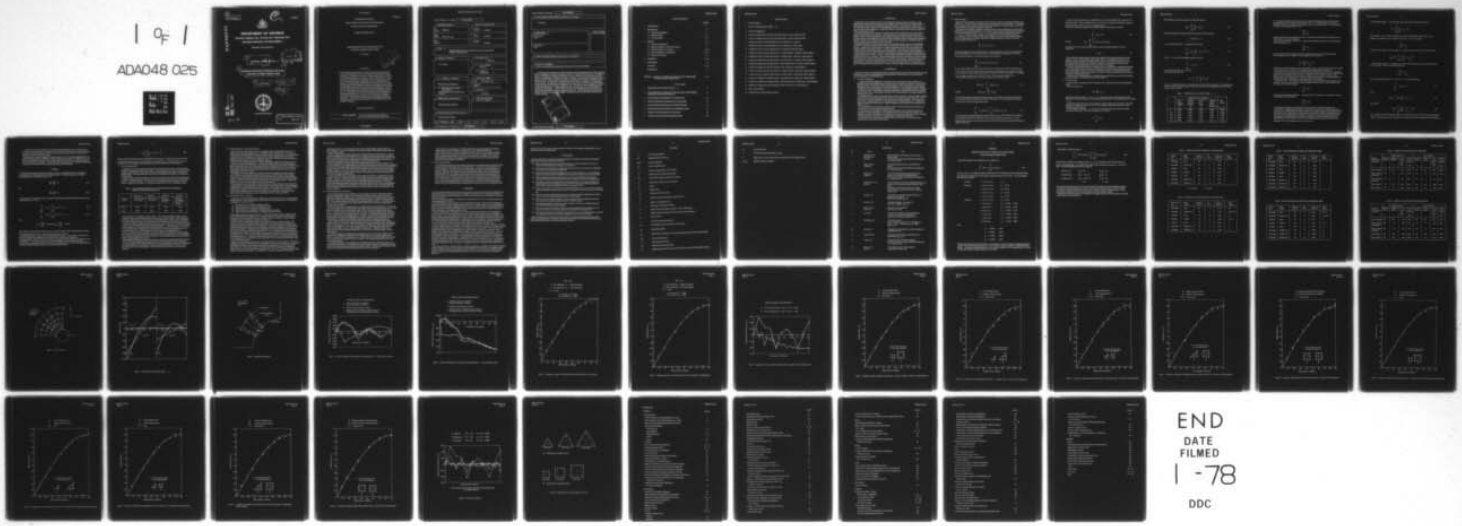

END
DATE FILMED
1-78
DDC

(14) WRE-TR-1810 (W)

AR-000-552

AUSTRALIA

DEPARTMENT OF DEFENCE

DEFENCE SCIENCE AND TECHNOLOGY ORGANISATION

WEAPONS RESEARCH ESTABLISHMENT

SALISBURY, SOUTH AUSTRALIA

(9) TECHNICAL REPORT, 1810 (W)

(6) IMPROVED INTEGRATION TECHNIQUES FOR FLUID FLOW FINITE ELEMENT FORMULATIONS

(10) C.A.J. FLETCHER

(11) Apr 77

(12) 47 p.

Approved for Public Release.

APRIL 1977

AR-000-552

DEPARTMENT OF DEFENCE

DEFENCE SCIENCE AND TECHNOLOGY ORGANISATION

WEAPONS RESEARCH ESTABLISHMENT

TECHNICAL REPORT 1810 (W)

IMPROVED INTEGRATION TECHNIQUES FOR FLUID FLOW FINITE ELEMENT FORMULATIONS

C.A.J. Fletcher

SUMMARY

Two refinements in the application of numerical integration, alternative sampling points and reduced integration, have been investigated for a Galerkin finite element formulation of a representative flow problem. By sampling the solution at the Gauss points a significant improvement in accuracy is achieved. The accuracy gain is lost if the solution at the Gauss points is extrapolated to the edge of the element. Consideration of a one-dimensional problem suggests that the use of reduced integration is equivalent to fitting the equation residual in the least-squares sense over each element. The employment of reduced integration, rather than exact integration, for incompressible, inviscid flow about a two-dimensional cylinder has produced solutions that are ten times more efficient if quadratic rectangular elements, either Serendipity or Lagrange, are used. The utilization of linear rectangular elements has caused a smaller improvement. The improvements associated with the introduction of reduced integration are independent of grid refinement. The use of reduced integration and triangular elements, with both linear and quadratic shape functions, has produced no significant improvement. The results herein reinforce the previously published conclusion that the quadratic, rectangular, Serendipity element is the most efficient element for flow problems of this type.

POSTAL ADDRESS: The Director, Weapons Research Establishment,
Box 2151, G.P.O., Adelaide, South Australia, 5001.

DOCUMENT CONTROL DATA SHEET

Security classification of this page: UNCLASSIFIED

1 DOCUMENT NUMBERS	2 SECURITY CLASSIFICATION
AR Number: AR-000-552	a. Complete Document: Unclassified
Report Number: WRE-TR-1810 (W)	b. Title in Isolation: Unclassified
Other Numbers:	c. Summary in Isolation: Unclassified

3 TITLE

IMPROVED INTEGRATION TECHNIQUES FOR FLUID FLOW FINITE ELEMENT FORMULATIONS

4 PERSONAL AUTHOR(S):

C.A.J. Fletcher

5 DOCUMENT DATE: April 1977

6 6.1 TOTAL NUMBER OF PAGES: 51

6.2 NUMBER OF REFERENCES: 13

7 7.1 CORPORATE AUTHOR(S):

Weapons Research Establishment

7.2 DOCUMENT (WING) SERIES AND NUMBER

Weapons Research and Development Wing TR-1810

8 REFERENCE NUMBERS

a. Task: DST 76/009 : (524)

b. Sponsoring Agency:

9 COST CODE: 239153/343

10 IMPRINT (Publishing establishment):

Weapons Research Establishment

11 COMPUTER PROGRAM(S) (Title(s) and language(s))

12 RELEASE LIMITATIONS (of the document):

Approved for Public Release.

12.0	OVERSEAS	NO		P.R.	1	A		B		C		D		E	

Security classification of this page: UNCLASSIFIED

Security classification of this page: UNCLASSIFIED

13 ANNOUNCEMENT LIMITATIONS (of the information on these pages):

No limitation

14 DESCRIPTORS:

a. EJC Thesaurus Terms

b. Non-Thesaurus Terms

15 COSATI CODES:

16 LIBRARY LOCATION CODES (for libraries listed in the distribution):

17 SUMMARY OR ABSTRACT:
(if this is security classified, the announcement of this report will be similarly classified)

Two refinements in the application of numerical integration, alternative sampling points and reduced integration, have been investigated for a Galerkin finite element formulation of a representative flow problem. By sampling the solution at the Gauss points a significant improvement in accuracy is achieved. The accuracy gain is lost if the solution at the Gauss points is extrapolated to the edge of the element. Consideration of one-dimensional problem suggests that the use of reduced integration is equivalent to fitting the equation residual in the least-squares sense over each element. The employment of reduced integration, rather than exact integration, for incompressible, inviscid flow about a two-dimensional cylinder has produced solutions that are ten times more efficient if quadratic rectangular elements, either Serendipity or Lagrange, are used. The utilization of linear rectangular elements has caused a smaller improvement. The improvements associated with the introduction of reduced integration are independent of grid refinement. The use of reduced integration and triangular elements, with both linear and quadratic shape functions, has produced no significant improvement. The results herein reinforce the previously published conclusion that the quadratic, rectangular, Serendipity element is the most efficient element for flow problems of this type.

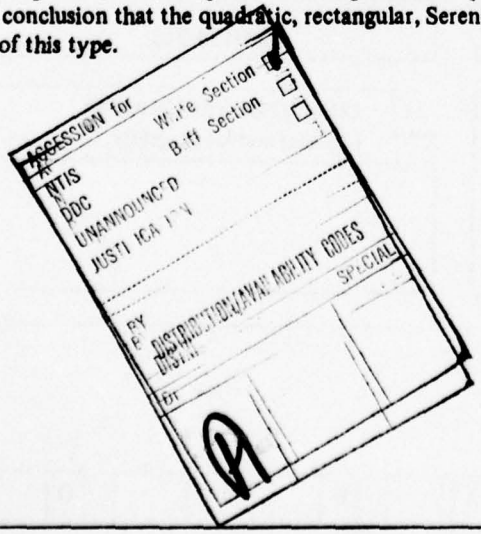

Security classification of this page: UNCLASSIFIED

TABLE OF CONTENTS

LIST OF TABLES

LIST OF FIGURES

1. INTRODUCTION

The application of the finite element method to fluid flow problems has been a fairly recent occurrence. Most applications so far have been aimed at demonstrating the possibility of obtaining solutions to fluid flow problems by the finite element method rather than obtaining the most efficient solution. As a consequence a number of the refinements that have been employed in structural applications of the finite element method to improve efficiency have yet to be tried on fluid flow applications. Computational efficiency is determined by the execution time required to achieve a predetermined accuracy.

The purpose of this report is to consider two such refinements, alternative sampling points and reduced integration, applied to a representative fluid flow problem. Both these refinements relate to the numerical integration that is necessary to convert the governing partial differential equations into governing algebraic equations. These concepts have been explored in such applications as the analysis of plates and shells(ref. 1 and 2), the smoothing of discontinuous stresses(ref.3) and the use of "thick shell" programs for solving thin shell problems(ref.4); a significantly improved efficiency, in the above sense, has been reported in many cases.

The representative fluid flow problem is the flow about a two-dimensional circular cylinder of an incompressible, inviscid fluid. This problem is chosen because it possesses an exact solution which permits a direct measure of the accuracy. A Galerkin finite element formulation in primitive variables has been used as this is more representative of general fluid flow problems than is the use of a variational principle. Previously the same model problem and formulation have been used to systematically assess the relative merits of various elements and shape functions(ref.5).

The plan of this report is as follows. In Section 2 some background developments of alternative sampling points and reduced integration are introduced. In Section 3 results for various sampling points with different orders of numerical integration are presented and compared. Additional results are given in Section 3 which illustrate an increased accuracy for the same execution time when reduced integration is used instead of full integration. The same elements and shape functions that were compared for full integration in reference 5 are compared for reduced integration in Section 3. This comparison considers both coarse and refined grids. In Section 4 the results of Section 3 are interpreted in the light of the background material given in Section 2. Section 5 contains an explicit list of the conclusions of this study.

2. BACKGROUND

In this section a little of the background development of alternative sampling points and reduced integration is set down. Although both concepts have been established qualitatively,published material indicates that very few quantitative results are applicable to other than specific cases.

2.1 Alternative sampling points

A typical finite element formulation (e.g. reference 5) converts a problem of continuous variables (e.g. u, v) governed by partial differential equations into a problem of discrete variables (e.g. nodal values $\bar{u}$, $\bar{v}$) governed by algebraic equations. This is done by arbitrarily approximating the continuous variables by low order, piecewise polynomials in which the nodal values are the unknown coefficients. To form the algebraic relations typically a weighted form of the governing equations(ref.6), with the polynomial approximations substituted, is integrated over the whole domain. If the integration is performed analytically the only approximation present is associated with forcing the solution to behave locally as though it were a low-order polynomial, assuming an isoparametric formulation is not used.

If the integration is performed numerically additional errors may be introduced. Numerical integration implicity fits a low order function, typically a polynomial, to the data and performs the integration analytically. The low order function fits the data by requiring an exact match at certain predetermined points. The numerical integration is then a weighted summation of the integrands evaluated at the predetermined points. Normally Gauss quadrature is used because with n points it is capable of integrating exactly integrands of polynomial form up to order 2n - 1(ref.7).

Thus normally the order of the numerical integration is chosen to be sufficiently high that the integration is exact for the order of the finite element representation used.

For problems that can be solved by formulating a variational principle it has been shown(ref.4) that at the Gauss points the differential expressions in the integrand are closer to the exact values then elsewhere. For example, for a cantilever beam subject to a distributed load the stresses are determined very accurately if sampled at the Gauss points but are very inaccurate and discontinuous if sampled at the nodal points.

In the present problem alternative points within the element are considered to see if consistently better agreement with the exact solution can be obtained.

2.2 Reduced integration

Reducing the order of integration below that required to make the integration exact necessarily introduces some additional error. Clearly if the order is reduced too much convergence may no longer be achieved. The minimum order of integration for convergence is that which permits exact integration of the element volume (or area in two dimensions) when an isoparametric formulation is used(ref.8).

The optimum order of integration depends on the order of the finite element representation, p, and the order of differentiation, d, in the governing equation. For problems of a variational nature such as the plane strain problem it has been deduced(ref.4) that for p = 1 and d = 1, 1 point integration formulae should be optional while for p = 2 and d = 1, 4 point integration formulae would be required if an element is considered in isolation.

If the stiffness matrix is considered as a whole, reduced integration may be viewed from a different perspective. Since the Galerkin method is an example of the Method of Weighted Residuals it is instructive to derive the governing algebraic equations from

$$\iint N_i \, . \, R \, . \, dx \, dy = 0, \tag{1}$$

where R is the residual of one of the equations after the analytic representation in terms of the nodal unknowns has been substituted (see reference 6 for more details). N_i is the shape function appropriate to the i^{th} node.

If the integration in equation (1) is carried out numerically then the result is

$$\sum_{k=1}^{M} W_k \, . \, N_i(x_k, y_k) \, . \, R(x_k, y_k) = 0. \tag{2}$$

W_k is the weight attached to the k^{th} function evaluation point. M is the number of function evaluation points, i.e. the produce of m function evaluation points per element and c contributing elements. Because of the nature of N_i only the four rectangular elements surrounding the i^{th} node will contribute to the summation. For example at node 1 in figure 1, only elements w, x, y and z contribute. Thus in any one equation $M \leqslant 4\,m$.

The residual R could depend on any of the n nodal unknowns, q_j, in the domain. Thus

$$R(x_k, y_k) = \sum_{j=1}^{n} R_j(x_k, y_k) \, . \, q_j \tag{3}$$

Typically $$R_j(x_k, y_k) = \frac{\partial N_j}{\partial x} \quad (x_k, y_k)$$

For convenience, elements are assumed to be perfectly regular. The symbol n is the product of the number of nodes n_n and the number of unknowns per node which in this case is 2. Certain of the q_j will be known and hence equation (2) with (3) substituted can be written.

$$\sum_{k=1}^{M} W_k \, . \, N_i(x_k \, y_k) \, . \sum_{j=1}^{L} R_j(x_k, y_k) \, . \, q_j = B_i, \tag{4}$$

where B_i represents the weighted summation associated with the known q_j. The problem now has L unknowns and L equations like (4) must be written down in order to obtain a unique solution for the q_j's. It is also apparent that for a solution to be possible, the total number of function evaluations M_T must not be less than the number of unknowns L.

Using exact numerical integration, M_T is much larger than L, using reduced integration M_T is much closer to L although still greater. There is a possibility that if L is too close to M_T a subsystem of [q] might be completely determined from a few elements; this is clearly a singular situation.

If the order of summation in equation (4) is reversed the familiar stiffness equation is obtained,

$$\sum_{j=1}^{L} K_{ij} \cdot q_j = B_i, \tag{5}$$

where K_{ij}

$$K_{ij} = \sum_{k=1}^{M} W_k \cdot N_i(x_k, y_k) \cdot R_{ij}(x_k, y_k) .$$

Consequently for a solution using reduced integration to lead a non-singular stiffness matrix [K], it is necessary that

$$e \cdot m > L \tag{6}$$

The use of reduced integration implies a fitting of the integrand with a lower order polynomial than that implied by the order of the finite element approximation. Hinton and Campbell(ref.3) prove that for two-dimensional parabolic isoparametric rectangular elements applied to a typical variational formulation of the finite element method, the use of reduced integration is equivalent to performing the integration exactly after applying a least squares bilinear fit separately to each term of the integrand.

Thus since the finite element formulation constrains the solution to locally follow a low-degree polynomial the *use of reduced integration may be thought of as relaxing some of the constraints on the solution at the expense* of introducing additional errors by not carrying out the integration exactly. The empirical evidence clearly indicates that the gains associated with relaxing the constraints far outweigh the losses associated with executing the numerical integration less accurately.

A fuller discussion of specific applications of reduced integration may be found in reference 4 and a discussion of reduced integration in a wider context may be found in reference 9.

2.3 A worked example

A simple example in one dimension will be considered in order to illustrate how and why reduced integration works.

The governing equation is

$$L(y) = \frac{dy}{dx} - y = 0, \tag{7}$$

subject to the boundary condition $y = 1$ at $x = 0$. It is of historical interest that this problem was used by Duncan(ref.10) to illustrate the classical Galerkin method (see also reference 6). This problem has the exact solution $y = e^x$.

A solution is sought for $0 \leqslant x \leqslant 1$ and five nodal values $\bar{y}$, at equal intervals of x, are introduced. The domain is split into two elements, $0 \leqslant x \leqslant 0.5$ and $0.5 \leqslant x \leqslant 1$, and quadratic Lagrange shape functions are used to determine the local variation of y.

From the boundary condition $\bar{y}_1 = 1$; hence only four independent equations are required to uniquely determine the unknown $\bar{y}_j$'s. The analytic representation of y is given by

$$y = \sum_{j=1}^{5} N_j \cdot \bar{y}_j . \tag{8}$$

Substituting this into equation (7) produces a residual, R(x), given by

$$R(x) = \sum_{j=1}^{5} \left\{ \frac{dN_j}{dx} - N_j \right\} \bar{y}_j . \tag{9}$$

Forming the integral of the weighted residual over the domain (see reference 6) gives

$$\int_0^1 W_i \, R(x) \, dx = 0. \tag{10}$$

For the Galerkin method $W_i = N_i$ and equation (10) becomes

$$\sum_{j=1}^{5} \int_0^1 N_i \left\{ \frac{dN_j}{dx} - N_j \right\} dx . \bar{y}_j = 0. \tag{11}$$

Setting i = 2 to 5 gives sufficient algebraic equations of the form

$$\sum_{j=1}^{5} a_{ij} . \bar{y}_j = 0. \tag{12}$$

to solve for the unknowns : $\bar{y}_2, \bar{y}_3, \bar{y}_4$ and $\bar{y}_5$.
The coefficients a_{ij} are given by

$$a_{ij} = \int_0^1 N_i \left\{ \frac{dN_j}{dx} - N_j \right\} dx \tag{13}$$

and are to be evaluated numerically. The integral is evaluated for each element separately. If a three point Gauss quadrature formula is used the integrations are performed exactly and the corresponding solution for the nodal values $\bar{y}_j$ are shown in Table 1.

TABLE 1. COMPARISON OF SOLUTIONS FOR $\frac{dy}{dx} - y = 0$

x	Approximate solution (nodal), $\bar{y}$				Exact solution
	Exact numerical integration $\bar{y}^{ei}$	Reduced numerical integration $\bar{y}^{ri}$	Local L.S. fit of residual $\bar{y}^{ls}$	Traditional Galerkin (quartic polynomial)	$y = e^x$
0	1.0000	1.0000	1.0000	1.0000	1.0000
0.25	1.2707	1.2838	1.2838	1.2840	1.2840
0.50	1.6403	1.6486	1.6486	1.6488	1.6487
0.75	2.0990	2.1165	2.1165	2.1170	2.1170
1.00	2.6938	2.7180	2.7180	2.7182	2.7183

If a two point Gauss quadrature (reduced integration) formula is used the integrations are not formed exactly; the corresponding results for the nodal values are shown in Table 1. It is self-evident that the use of reduced integration, rather than exact integration, has produced a very much more accurate solution. It would be possible to construct a local least-squares fit to the term

$$\left\{ \frac{dN_j}{dx} - N_j \right\}$$

in equation (13) and carry out the integration exactly. If this were done the results would be identical to those shown in Table 1 under reduced integration.

This is because the least-squares fit of order n - 1 always cuts the original curve of order n at the n Gauss points. Thus the least-squares fit of

$$\left\{ \frac{dN_j}{dx} - N_j \right\}$$

over each element would be a straight line cutting the original quadratic function at the two Gauss points. Since the weight function N_i is quadratic, the total integration, over each element, of

$$\int_0^1 N_i \left\{ \frac{dN_j}{dx} - N_j \right\}_{ls} dx$$

could be carried out exactly using a two point Gauss quadrature formula. Thus the sampling values of the integrand would be exactly the same as for the reduced integration of the original expression in equation (13).

Also shown in Table 1 are results for a traditional Galerkin formulation(ref.6) in four unknowns. It is generally found that because the analytic representation and the weighting functions are allowed to span the complete domain superior results are obtained(ref.6) with the traditional Galerkin method than with a finite element or finite difference method with the same number of unknowns. Table 1 indicates that the use of reduced integration has produced results that are almost as good as using a traditional Galerkin formulation.

The question remains: why does the use of reduced integration give more accurate results than the use of exact integration? The answer can be found by pursuing the equivalence between the use of reduced integration and the least squares fitting of the expression

$$\left\{ \frac{dN_j}{dx} - N_j \right\}$$

in equation (13) and subsequent integration. If equations (13), (12), (11) and (10) are considered it is clear that the least-squares fit of the expression

$$\left\{ \frac{dN_j}{dx} - N_j \right\}$$

over each element is equivalent to a least-squares fit over each element of the residual in equation (10).

The basis for the weighted residual method(ref.6) is that, since the introduction of an analytic representation produces a non-zero residual equation throughout the domain, a reasonable approximate solution will be obtained if the residual is made to equal zero in some global sense e.g. equation (10). Ideally the residual should be zero everywhere. If the weight function is predominantly of one sign the variation of R may be expected to include some changes of sign if equation (10) is to be satisfied. Therefore a low order least-squares fit of R whose weighted integral over the domain is zero is likely to have local magnitudes of R_{ls} that are less than the local magnitudes of R, and hence produce a solution closer to the exact.

This is illustrated in figure 2. From the solution using exact numerical integration the expression

$$R_{ei} = \sum_{j=1}^{5} \left\{ \frac{dN_j}{dx} \cdot N_j \right\} \cdot \bar{y}_j^{ei}$$

has been plotted. R_{ei} is the equation residual corresponding to the approximate solution, $\left\{ \bar{y}_j^{ei} \right\}$ R_{ei} is quadratic in x and discontinuous at the element boundary (x = 0.5). If the expression

$$\left\{ \frac{dN_j}{dx} \cdot N_j \right\}$$

in equation (13) is fitted by a linear least-squares curve a pseudo-residual, based on $\bar{y}_j^{ei}$, can be constructed as

$$R_{ls}(\bar{y}_j^{ei}) = \sum_{j=1}^{5} \left\{ \frac{dN_j}{dx} \cdot N_j \right\}_{ls} \bar{y}_j^{ei} .$$

This is also plotted in figure 2. It is apparent that the effect of the least-squares fit has not greatly reduced the size of the residual. However the residual (R_{ls}), based on

$$\left\{ \frac{dN_j}{dx} \cdot N_j \right\}_{ls}$$

and the corresponding solution $\bar{y}_j^{ls}$, is much smaller. $\bar{y}_j^{ls}$ is obtained by solving

$$\sum_{j=1}^{5} (a_{ij})_{ls} \cdot \bar{y}_j = 0, \qquad (16)$$

where

$$(a_{ij})_{ls} = \int_0^1 N_i \left\{ \frac{dN_j}{dx} \cdot N_j \right\}_{ls} dx. \qquad (17)$$

R_{ls} is given by

$$R_{ls} = \sum_{j=1}^{5} \left\{ \frac{dN_j}{dx} \cdot N_j \right\}_{ls} \cdot \bar{y}_j^{ls} . \qquad (18)$$

R_{ls} is actually zero but has been plotted in figure 2 in order that it will show up. Because of the local least-squares fit R_{ls} is a linear function of x, R_{ls} is identical with the residual obtained from a reduced integration formulation, R_{ri}.

The lower the order of the least-squares fit the closer the residuals should be to zero. However as noted previously the total number of function evaluations in the domain must not be less than the number of unknowns. In the present example the number of unknowns is four, there are two elements, therefore a two point Gauss quadrature formula is the lowest order possible.

This interpretation of reduced integration clearly points towards the use of a least-squares approximation to the method of weighted residuals or an MWLSR as a valuable technique in its own right. The "magic" in the use of a lower order Gauss quadrature formula is that it permits a shortcut to be taken so that the least-squares approximation to the residual is set up implicitly. Thus the use of Gauss quadrature formulae is convenient but not essential to the success of a solution after approximating the residual in the least-squares sense.

3. RESULTS

The model fluid flow problem considered in this report is inviscid, incompressible flow about a two-dimensional circular cylinder; the flow-field is represented schematically in figure 1. The governing equations, for inviscid, incompressible flow in two dimensions, are taken to be

$$\frac{\partial u}{\partial x} + \frac{\partial v}{\partial y} = 0 \tag{19}$$

and

$$\frac{\partial u}{\partial y} - \frac{\partial v}{\partial x} = 0 . \tag{20}$$

After application of a Galerkin finite element formulation the governing partial differential equations can be reduced to algebraic equations of the form

$$\sum_{j=1}^{n} a_{ij} \cdot \bar{u}_j + \sum_{j=1}^{n} b_{ij} \cdot \bar{v}_j = 0, j = 1, n \tag{21}$$

$$\sum_{j=1}^{n} b_{ij} \cdot \bar{u}_j - \sum_{j=1}^{n} a_{ij} \cdot \bar{v}_j = 0, j = 1, n, \tag{22}$$

where

$$a_{ij} = \iint \frac{\partial N_j}{\partial x} \cdot N_i \, dxdy \text{ and } b_{ij} = \iint \frac{\partial N_j}{\partial y} \cdot N_i \, dxdy.$$

The symbols $\bar{u}_j$, $\bar{v}_j$ represent the nodal values of u and v, n is the total number of nodal unknowns and N_i is the shape function associated with the i^{th} node. Further details may be found in reference 5.

A computational solution is sought within the region ABCD shown in figure 1. The nodal points and elements are defined on a polar grid and an isoparametric formulation is used to connect this to a cartesian grid.

All results presented in this section are for the variation of the tangential velocity component at the body surface with angular position. As in reference 5 it is felt that this represents a stringent test of the computational results.

In order to have a single number represent the accuracy of the computational results, the root mean square difference, σ, between the finite element solution and the exact solution is defined as follows

$$\sigma = \left[\left\{ \sum_{i=1}^{N} (q_T - q_e)^2 \right\} / N \right]^{\frac{1}{2}} , \qquad (23)$$

where q_T is the finite element solution for the tangential velocity component. The symbol, q_e is the exact solution for the tangential velocity component and N is the number of nodes between $\theta = 0^o$ and 90^o (B and C in figure 1). The symbol, σ may be thought of as the average difference between the computational and exact solutions.

3.1 Alternative sampling points

From Section 2.1 it is to be expected that the solution at the Gauss points will be closer to the exact solution calculated at the Gauss points than the nodal solution is to the exact solution at the nodes. For practical purposes the solution at the body surface is of interest. The body surface coincides with the boundary of a number of adjacent elements. Thus nodal values at the body surface are available but the Gauss points do not coincide with the body surface.

Using the analytic representation implicit in the finite element formulation the solution at the Gauss points can be obtained. Using just the solution at the Gauss points an extrapolation is made onto the body surface as shown in figure 3. This gives the solution C. The nodal solution B is interpolated along the body surface to give the solution D which is at the same point as C. This process is repeated for 2 x 2 and 3 x 3 integration formulae.

TABLE 2. R.M.S. ERRORS FOR ALTERNATIVE SAMPLING POINTS AND DIFFERENT NUMERICAL INTEGRATION FORMULAE

	Solution A	Solution B	Solution C	Solution D
Integration formula	R.M.S. difference at Gauss points	R.M.S. difference at nodal points	Solution A extrapolated to the surface	Solution B interpolated to same position as Solution C
4 point	0.085	0.017	0.016	0.015
9 point	0.009	0.062	0.066	0.058

The results for the r.m.s. differences are shown in Table 2. These results were obtained using second order rectangular elements of the Serendipity type with 149 unknowns in the whole flow-field. The actual differences between the computed and exact solutions are plotted against angular position in figures 4 and 5 corresponding to the different integration formulae. On each of figures 4 and 5 the solutions B, C and D (figure 3) are shown.

Examination of Table 2 indicates that the solution at the Gauss points is better for the 3 x 3 integration formulae, i.e. the lowest order that still performs the numerical integration exactly. This solution, using a 3 x 3 integration formula is superior to the nodal point solution using reduced integration. Once the Gauss point solution, for the 3 x 3 integration formula, is extrapolated to the surface (Solution C in Table 2) the increased accuracy of the Gauss point solution is lost. In fact all solutions at the body surface are of comparable accuracy.

The use of a reduced integration formula (2 x 2) produces a relatively inaccurate solution at the Gauss points (Solution A) but a very accurate solution when extrapolated to the body surface (Solution C). The interpolation of the nodal point solution (Solution D) to the same position as the extrapolated Gauss point solution (Solution C) has always produced a slightly better solution.

Both integrating formulae (figures 4 and 5) produce solutions which show some disagreement between solutions C and D at the forward stagnation point but good agreement as the shoulder point ($\theta = 90^o$) is approached.

The general conclusion of these results is that the use of alternative sampling points (Solutions C and D) produces only marginal improvement in accuracy when compared with the large improvement in accuracy at the nodes associated with the use of reduced integration. Comparable results were obtained when a refined grid was considered.

3.2 Reduced integration vs. conventional integration

Solutions have been obtained using a second order rectangular element of the Serendipity type with a 2 x 2 integration formula (reduced integration) and a 3 x 3 integration formula (full integration). The results for a coarse grid (149 nodal unknowns in the flow field) are shown in figure 6. Because of the use of a dummy element to carry out the numerical integration (see reference 5) the use of reduced integration has not produced any significant improvement in execution time (as suggested in reference 4). Therefore any execution time shown is nominally the same irrespective of the order of numerical integration.

The results for the coarse grid indicate that the solution using reduced integration is more than three times as accurate as the solution using full integration. An examination of figure 6 indicates that the full integration solution always lies below the exact solution whereas the reduced integration solution straddles the exact solution. Thus an additional advantage of the reduced integration solution, not apparent from the r.m.s. error results, is the possibility of fitting a low order least squares curve through the reduced integration results to obtain even better agreement with the exact results.

The possibility exists that the improvement produced by using reduced integration will lessen as the grid is refined. Results for a moderately refined grid (299 nodal unknowns in the flow field) are shown in figure 7. As is apparent the reduced integration solution is still better than three times as accurate as the full integration solution. A further refinement in the grid (with 582 nodal unknowns in the flow field) also produced a reduced integration solution that was better than three times as accurate as the full integration solution. Because both solutions are very close to the exact solution this case has not been plotted.

A better appreciation of the improvements associated with the use of reduced integration may be obtained by considering figure 8. The reduced integration results correspond to those plotted in figure 6; the full integration results have been obtained by refining the grid until a solution of the same total accuracy is produced. It may be noted that this has required more than ten times the execution time. By plotting the tangential velocity differences against angular position the tendency for the full integration solution to underestimate the exact solution and the reduced integration solution to straddle the exact solution is made more obvious.

3.3 Reduced integration on a coarse grid

In this section various element/shape function combinations are compared for solutions on a coarse grid using reduced integration. The same element/shape function combinations are considered here as were considered for full integration in reference 5, namely:

(1) linear shape function in triangular isoparametric element
(2) quadratic shape function in triangular isoparametric element
(3) linear shape function in rectangular isoparametric element
(4) quadratic shape function (Lagrange) in rectangular isoparametric element
(5) quadratic shape function (Serendipity) in rectangular isoparametric element

All these shape functions are described in reference 11. The various numerical integration formulae used with various element/shape function combinations are described in Appendix I. However the results presented in this section cannot be compared with those given in reference 5 since the grid used here is coarser; the grids considered in reference 5 correspond to the grids used in Section 3.4.

Results for linear and quadratic shape functions, for rectangular elements, are compared in figure 9. The numerical integrations for the quadratic shape functions have been evaluated with a 4 point formula based on evaluating the integrands at the Gauss points (see Appendix I). The numerical integrations for the linear shape functions have been evaluated with a 1 point formula based on evaluating the integrands at the mid point of the elements (see Appendix I). Although both solutions straddle the exact solution the solution using a quadratic shape function is noticeably smoother particularly close to $\theta = 90^{\circ}$. As is apparent from Table 4 the solution, using quadratic shape functions of the Serendipity type, is approximately twice as accurate as the solution using linear shape functions. The solution using quadratic shape functions is also more economical, mainly because it has less nodal unknowns. A comparison of Tables 3 and 4 indicates that the use of reduced integration in place of exact integration (3 x 3 formula) causes a greater improvement in accuracy for quadratic shape functions than it does for linear shape functions.

Results for linear and quadratic shape functions, for triangular elements, are shown in figure 10. The numerical integrations for the quadratic shape functions have been evaluated using a 4 point formula given by Cowper(ref.12). The numerical integration for the linear shape functions have been evaluated with a 1 point formula given by Zienkiewicz(ref.11). Examination of figure 10 and Table 4 indicates that the results for linear elements are closer to the exact solution on average but become rather poor close to $\theta = 90^{\circ}$. The solution using linear shape functions is exactly the same whether a 1 point (Table 4) or 7 point (Table 3) integration formula is used.

This indicates that use of a 1 point integration formula is exact for linear triangular elements applied to the present problem. The use of reduced integration for a quadratic triangular element produces some improvement in accuracy (Tables 3 and 4).

Results for triangular and rectangular elements, with linear shape functions are shown in figure 11. Since the results with triangular elements are exact with the use of a one point integration formula the results generally lie beneath the exact results whereas the results for the use of rectangular elements straddle the exact solution. Both sets of results have the same number of nodal unknowns and hence approximately the same CPU time but the solutions using rectangular elements are approximately twice as accurate (see Table 4).

Results for triangular and rectangular elements, with quadratic shape functions are shown in figure 12. The numerical integrations for the quadratic shape functions have been evaluated with a 4 point formula (see Appendix I). The results for the rectangular elements (Lagrange shape function) lie much closer to the exact solution (figure 12) particularly close to $\theta = 90^{o}$. Both solutions required approximately the same CPU time but the results using rectangular elements are almost three times as accurate on average. The use of reduced integration for quadratic rectangular elements of the Lagrange family has produced a two-fold improvement in accuracy compared with the use of exact integration (Tables 3 and 4).

Quadratic rectangular elements of the Lagrange and Serendipity families have been compared and the results are shown in figure 13. The grids and number of unknowns have been adjusted to give approximately the same CPU time. As can be seen from figure 13 the results using quadratic shape functions of the Serendipity family lie substantially closer to the exact solution than the results using a Lagrange shape function. The average accuracy using Serendipity shape functions is approximately three times greater than the accuracy using Lagrange shape functions for comparable CPU times (Table 4). Both types of shape function, with reduced integration, produce results that straddle the exact solution and hence could be made to produce better agreement by a low order least squares fit.

3.4 Reduced integration on a moderate grid

The same element/shape function combinations, as set out in Section 3.3, are here compared for solutions on moderate grids using reduced integration. The detailed results are shown in figures 14 to 18 and the gross properties of the solutions are listed in Table 6. Comparative results using exact integration are given in Table 5. Many of these results have been obtained using the same grids as in reference 5. However the results shown in Table 5 have required considerably less CPU time than the results presented in reference 5. This improvement in efficiency is due to system changes to the computer (IBM 370/168) used to obtain the results rather than to improvements in this program.

Results for linear and quadratic shape functions, for rectangular elements, are shown in figure 14. The solution using quadratic shape functions of the Serendipity type is closer to the exact solution particularly close to $\theta = 90^{o}$. However the general character of both solutions is similar to that of the solutions using coarse grids shown in figure 9. Comparison of Tables 4 and 6 indicates that the solution using quadratic shape functions is approximately twice as accurate as the corresponding solution on a coarse grid. The results using linear shape functions are also more accurate than the corresponding results on a coarse grid. Also both linear and quadratic solutions are considerably more accurate than corresponding solutions (Table 5) obtained using an exact integration formula (see Appendix I) on a moderate grid, although the improvement is greater for quadratic shape functions.

Linear and quadratic shape functions used with triangular elements have been compared and the results are presented in figure 15. The results are of approximately the same accuracy although the solution using quadratic elements is more accurate close to $\theta = 90^{o}$. Both solutions are considerably more accurate than those obtained using a coarse grid (figure 10). As with the coarse grid solutions, the results using a linear shape function are exactly the same whether a 1 point or 7 point integration formula is used. Comparison of Tables 5 and 6 indicates that the solution using quadratic shape functions is less accurate with reduced integration than with exact integration.

The results for triangular and rectangular elements using linear shape functions are shown in figure 16 and it is apparent that the rectangular element solution is considerably more accurate. Since the triangular element solution is the same whether the integration is exact or reduced and since both elements produce results of equal average accuracy when the integration is exact, any superiority of the rectangular element must be due to the use of reduced integration.

A comparison of results for the use of triangular and rectangular elements with quadratic shape functions on a moderate grid indicates (figure 17 and Table 6) that the use of rectangular elements of the Lagrange type produces results that are three times as accurate as those using triangular elements. This improvement in accuracy is of the same order as was obtained with coarse grids using both exact and reduced integration.

However the use of exact integration on a moderate grid produces more accurate results with a quadratic triangular element than with a quadratic rectangular element of the Lagrange family (Table 5).

Figure 18 shows results of a comparison of quadratic rectangular elements of the Serendipity and Lagrange families. Both sets of results lie close to the exact solution; an examination of Table 6 indicates that the solution using Serendipity elements is more accurate. Both solutions are considerably more accurate than corresponding solutions using exact integration (Table 5) and more accurate than corresponding solutions obtained on a coarse grid (figure 13 and Table 4).

3.5 Effect of grid refinement

Solutions have been obtained for various meshes using isoparametric rectangular elements with quadratic shape functions of the Serendipity family and using reduced integration. The results for three representative cases are shown in figure 19. The results using a coarse mesh required the solution of 149 nodal unknowns and required 4.5 s CPU time; the results for a moderate mesh required the solution of 299 nodal unknowns and required 15 s CPU time and the results for a refined mesh required the solution of 582 nodal unknowns and required 69 s CPU time. As is apparent from figure 19 all three solutions straddle the exact solution and so could be made to agree with the exact solution even better by curve fitting the data in the least-squares sense with a low order function. These results indicate that the accuracy increases with the square root of the CPU time i.e. to double the accuracy requires four times the CPU time. Examination of figure 19 indicates that the use of the coarsest grid shown produces average differences that are less than 1% of the maximum velocity whilst use of the most refined grid produces average differences that are less than 0.2% of the maximum velocity.

4. DISCUSSION

Since flow problems normally require the solution on the element boundary it appears that alternative sampling points within the element, e.g. the Gauss points, offer no advantage over the nodal points. As is apparent from Section 3.1, if the solution at the Gauss points is extrapolated to the element boundary the accuracy is not significantly better than obtained at the nodes.

This section will be mainly devoted to a consideration of the results of Sections 3.2 to 3.4 in the light of some of the ideas underlying reduced integration.

The worked example considered in Section 2.3 used a quadratic shape function. The equivalent two-dimensional shape function would be a quadratic Lagrange shape function used in a rectangular element. The use of an isoparametric formulation and distorted elements probably degrades the accuracy to be expected from a four point Gauss quadrature formula. However, as is apparent from Section 3, the use of reduced integration produces considerable improvement. Similar remarks apply to the Serendipity quadratic element.

The linear rectangular element also produces more accurate results when reduced integration (one sampling point per element) is used. However the improvement over the use of exact integration is not as good as for quadratic rectangular elements. This is in spite of the fact that the ratio of function evaluation points per unknown is the same as for the use of Lagrange quadratic rectangular elements (Tables 7 and 8). Strang and Fix(ref.13) indicate that the use of one integration point with a linear shape function over a single element leads to an indefinite result, and caution against its use. Even though typical results with a linear rectangular element and reduced integration produced a smaller r.m.s. error than the use of exact integration the solution was often physically unsatisfactory (e.g. figure 14).

The use of reduced integration with triangular elements appears from this study to be relatively ineffective. In general terms, since triangular elements do not require as many unknown parameters they do not admit as many higher order terms as rectangular elements, and hence are more likely to be integrated with low order formulae. This is the case for linear triangular elements where even one sampling point per element is sufficient to produce exact integration. This is supported by the relatively large number of function evaluation points per unknown (see Tables 7 and 8). The case of quadratic triangular elements is inconclusive. The use of a four point integration formula certainly doesn't produce exact integration. However the interpretation of the sampling points as giving rise to a special fit (e.g. least-squares) of the residual is lacking for triangular elements. Consequently, perhaps it is not surprising that the use of a four point integration formula has not produced better results than the use of a seven point formula on average. In some instances the results were significantly worse. The question as to whether a symmetric four point formula exists that possesses a comparable interpretation to that of a four point Gauss quadrature formula for rectangular elements, deserves further study.

If the reason for the success of reduced integration is temporarily disregarded it is apparent that the ability of rectangular elements to respond to the use of reduced integration makes them significantly more efficient than triangular elements. The results of Section 3 indicate that the quadratic Serendipity element is more efficient than the quadratic Lagrange element and both are more efficient than the linear element. This order of merit is consistent with the results of reference 5.

The present study does not alter the general conclusion of reference 5 that the quadratic triangular element is more efficient than the linear triangular element.

5. CONCLUSIONS

From the present study of a Galerkin finite element formulation for a representative example of incompressible inviscid flow, the following conclusions have been drawn:

(a) With exact numerical integration the finite element solution is in much closer agreement with the exact solution at the Gauss integration points than at the nodal points.

(b) If the solution at the Gauss points is extrapolated to the edge of the element the solution is not significantly more accurate than the solution at the nodal points.

(c) Results for a one-dimensional problem suggest that the use of reduced integration, i.e. a lower order Gauss quadrature formula, is equivalent to fitting the equation residual in a least-squares sense over each element.

(d) Reduced integration has produced results that are as accurate as those produced by exact integration requiring ten times the CPU time, when used with quadratic rectangular elements of the Serendipity type.

(e) When applied to quadratic rectangular elements of the Lagrange type, the use of reduced integration has produced solutions of sufficient accuracy to require from 5 to 10 times as much CPU time, depending on grid refinement, to produce comparable results when exact integration is used.

(f) The use of a four point integration formula has produced inferior results to the use of a seven point integration formula when quadratic triangular elements are used on a refined grid. However the converse is true for coarse grid.

(g) The use of a one point integration formula with linear rectangular elements has produced superior results to the use of a four or nine point integration formula with the same elements.

(h) The use of a one point integration formula with linear triangular elements has produced exactly the same result as the use of a seven point integration formula with the same elements.

(i) The improvement associated with the use of reduced integration on Serendipity, rectangular elements has been found to be independent of grid refinement.

(j) The lack of success of reduced integration applied to quadratic triangular elements is probably due to the failure of the integration formula used to approximate the residual in the least-squares sense.

(k) The effectiveness of quadratic, rectangular, Serendipity elements for the use of reduced integration is consistent with comparable results obtained from structural applications of the finite element method.

This study indicates that the combination of reduced integration and quadratic Serendipity elements will permit accurate computational results to be obtained for flows about three-dimensional bodies with much coarser grids, and hence smaller execution times, than would have been possible otherwise.

NOTATION

A	area of triangle, Appendix I
B_i	weighted integral over known q_j's
CPU	central processing unit
K_{ij}	term in the stiffness matrix
L	number of nodal unknowns to be determined
M	number of function evaluations per equation
M_T	total number of function evaluations in the domain
N	shape function, number of points on the body
R	residual
W	weight function
a_{ij}	coefficient in the solution matrix
b_{ij}	coefficient in the governing algebraic equation, Section 3
c	number of contributing elements
e	total number of elements in the domain
m	number of function evaluations per element; order of differentiation
n	number of points in the integration formula; number of nodal unknowns
n_n	number of nodes
p	order of finite element representation
q_e	exact tangential velocity component at the body surface
q_j	typical nodal unknown
q_T	tangential velocity component at the body surface calculated from the finite element solution
[q]	vector of nodal unknowns
u, v	velocity components, figure 1
$\bar{u}, \bar{v}$	nodal values of velocity components
w_k	weight associated with the function value at the k^{th} point in the numerical integration formula

x, y	cartesian coordinates
σ	root mean square difference between q_T and q_e
θ	angular position around a circular cylinder, measured from the front stagnation point
ξ_i, η_i, ζ_i	triangular coordinates, Appendix I

REFERENCES

No.	Author	Title
1	Zienkiewicz, O.C., Taylor, R.L. and Too, J.M.	"Reduced Integration Techniques in General Analysis of Plates and Shells" International Journal for Numerical Methods in Engineering, Vol. 3, pp275-290,1971
2	Pawsey, S.F. and Clough, R.W.	"Improved Numerical Integration of Thick Shell Finite Elements" International Journal for Numerical Methods in Engineering, Vol. 3, pp575-586, 1971
3	Hinton, E. and Campbell, J.	"Local and Global Smoothing of Discontinuous Finite Element Functions using a Least Squares Method" International Journal for Numerical Methods in Engineering, Vol. 8, pp461-680, 1974
4	Zienkiewicz, O.C. and Hinton, E.	"Reduced Integration, Function Smoothing and Nonconformity in Finite Element Analysis (with special reference to Thick Plates)" Proceedings of the International Conference on Finite Element Methods in Engineering, University of Adelaide, December 1976
5	Fletcher, C.A.J.	"The Application of the Finite Element Method to Two-Dimensional, Inviscid Flow" WRE-TN-1606 (WR&D), May 1976
6	Fletcher, C.A.J.	"The Galerkin Method : An Introduction" WRE-TM-1632 (WR&D), June 1976
7	Isaacson, E. and Keller, H.B.	"Analysis of Numerical Methods" Wiley, New York, 1966
8	Irons, B.M.	"Finite Element Techniques in Structural Mechanics" Discussion H, Tottenham and Brebbia (Eds.), Southampton University Press, pp328-331, 1970
9	Zienkiewicz, O.C.	"Why Finite Elements" in Finite Elements in Fluids, Vol. 1, Ed. Gallagher, R.A., Oden, J.T., Taylor, C. and Zienkiewicz, O.C., Wiley, pp1-23, 1975
10	Duncan, W.J.	"Galerkin's Method in Mechanics and Differential Equations" ARC R&M 1798, 1937
11	Zienkiewicz, O.C.	"The Finite Element Method in Engineering Science" McGraw-Hill, London, 1971
12	Cowper, G.R.	"Gaussian Quadrature Formulas for Triangles" International Journal for Numerical Methods in Engineering, Vol. 4, pp405-408, 1972
13	Strang, G. and Fix, G.J.	"An Analysis of the Finite Element Method" Prentice-Hall, New Jersey, 1973

APPENDIX I

NUMERICAL INTEGRATION FORMULAE FOR VARIOUS SHAPE FUNCTION/ELEMENT COMBINATIONS

The numerical integration over a triangle of area A is obtained from

$$\iint f\,dA = A \sum_{i=1}^{n} w_i \cdot f(\xi_i, \eta_i, \zeta_i), \qquad (I.1)$$

where ξ_i, η_i and ζ_i are triangular coordinates associated with the i^{th} sampling point and w_i is the associated weight. The coordinates and weights of the various triangular integration formulae are set our below. The various sampling points are shown in figure 20

one point,	$a = \{1/3, 1/3, 1/3\}$,	$w_a = 1$
four-point,	$a = \{1/3, 1/3, 1/3\}$,	$w_a = -27/48$
	$b = \{3/5, 1/5, 1/5\}$,	$w_b = 25/48$
	$c = \{1/5, 3/5, 1/5\}$,	$w_c = 25/48$
	$d = \{1/5, 1/5, 3/5\}$,	$w_d = 25/48$
seven-point,	$a = \{1/3, 1/3, 1/3\}$,	$w_a = 0.225$
	$b = \{\alpha_1, \beta_1, \beta_1\}$,	$w_b = 0.13239\ 41528$
	$c = \{\beta_1, \alpha_1, \beta_1\}$,	$w_c = 0.13239\ 41528$
	$d = \{\beta_1, \beta_1, \alpha_1\}$,	$w_d = 0.13239\ 41528$
	$e = \{\alpha_2, \beta_2, \beta_2\}$,	$w_e = 0.12593\ 91805$
	$f = \{\beta_2, \alpha_2, \beta_2\}$,	$w_f = 0.12593\ 91805$
	$g = \{\beta_2, \beta_2, \alpha_2\}$,	$w_g = 0.12593\ 91805$

where

$\alpha_1 = 0.05971\ 58718$

$\beta_1 = 0.47014\ 20641$

$\alpha_2 = 0.79742\ 69854$

$\beta_2 = 0.10128\ 65073$

The seven-point formula has been used to produce exact integration for the linear and quadratic triangular isoparametric elements. The four-point formula has been used to carry out reduced integration of quadratic triangular isoparametric elements. The one-point formula has been used to carry out reduced integration of linear triangular elements. However the one-point formula produces exact integration for this problem.

Gauss quadrature formulae of the form

$$\int_{-1}^{1}\int_{-1}^{1} f(\xi,\eta)\, d\xi . d\eta = \sum_{i=1}^{n}\sum_{j=1}^{n} H_i . H_j . f(\xi_i,\eta_j) \qquad (I.2)$$

have been used to integrate f over rectangular elements. ξ_i, η_j are the coordinates of the i, j^{th} point and H_i, H_j are the corresponding weights. The coordinates and weights for Gauss quadrature formulae up to n = 3 are set out below. The various sampling points are shown in figure 20.

one-point (n=1)	$\xi_i, \eta_j = 0.0$	$H_i, H_j = 2.0$
four-point (n=2)	$\xi_i, \eta_j = \pm 1/\sqrt{3}$	$H_i, H_j = 1.0$
nine-point (n=3)	$\xi_i, \eta_j = \pm\sqrt{3}/\sqrt{5}$	$H_i, H_j = 5/9$
	$= 0.0$	$= 8/9$

The nine-point formula has been used to produce exact integration for quadratic rectangular isoparametric elements of both the Serendipity and Lagrange kind. The four-point formula has been used to carry out reduced integration over quadratic rectangular isoparametric elements and exact integration over linear rectangular elements. The one point formula has been used to carry out reduced integration over linear rectangular elements.

The definition of the coordinates used in the triangular and rectangular elements and a fuller description of numerical integration may be found in reference 11.

TABLE 3. EXACT INTEGRATION FORMULAE ON COARSE GRIDS

Element type	Shape function	Number of unknowns	CPU time (s)	Nodal r.m.s. difference	Figure reference
Rectangular	Linear	199	5.1	0.043	
Rectangular	Quadratic (S)	149	4.5	0.049	6
Triangular	Linear	279	8.5	0.040	
Triangular	Quadratic	199	7.1	0.120	
Triangular	Linear	199	5.1	0.061	
Rectangular	Quadratic (L)	199	7.5	0.047	
Rectanguiar	Quadratic (L)	159	5.0	0.071	

S = Serendipity L = Lagrange

TABLE 4. REDUCED INTEGRATION FORMULAE ON COARSE GRIDS

Element type type	Shape function	Number of unknowns	CPU time (s)	Nodal r.m.s. difference	Figure reference
Rectangular	Linear	199	5.3	0.033	9, 11
Rectangular	Quadratic (S)	149	4.5	0.015	6,8,9,13,19
Triangular	Linear	279	8.5	0.040	10
Triangular	Quadratic	199	7.3	0.060	10, 12
Triangular	Linear	199	5.1	0.061	11
Rectangular	Quadratic (L)	199	7.7	0.022	12
Rectangular	Quadratic (L)	159	5.1	0.042	13

TABLE 5. EXACT INTEGRATION FORMULAE ON MODERATE GRIDS

Element type	Shape function	Number of unknowns	CPU time (s)	Nodal r.m.s. difference	Figure reference
Rectangular	Linear	399	18	0.034	
Rectangular	Quadratic (S)	299	15	0.023	7
Triangular	Linear	599	34	0.024	
Triangular	Quadratic	399	23	0.018	
Triangular	Linear	399	17	0.034	
Rectangular	Quadratic (L)	399	25	0.023	
Rectangular	Quadratic (L)	319	16	0.025	
Rectangular	Quadratic (S)	582	65	0.013	

TABLE 6. REDUCED INTEGRATION FORMULAE ON MODERATE GRIDS

Element type	Shape function	Number of unknowns	CPU time (s)	Nodal r.m.s. difference	Figure reference
Rectangular	Linear	399	17	0.022	14, 16
Rectangular	Quadratic (S)	299	15	0.0071	7,14,18,19
Triangular	Linear	599	33	0.024	15
Triangular	Quadratic	399	22	0.026	15, 17
Triangular	Linear	399	16	0.034	16
Rectangular	Quadratic (L)	399	25	0.0072	17
Rectangular	Quadratic (L)	319	17	0.0080	18
Rectangular	Quadratic (S)	582	69	0.0035	19

TABLE 7. DEGREE OF DEFINITENESS FOR COARSE MESH

Element/ shape function combination	Reduced integration				Exact integration			
	Number of unknowns L	Number of elements e	No. of function eval. points M_T	Function eval. per unknown M_T/L	Number of unknowns L	Number of elements e	No. of function eval.. points M_T	Function eval. per unknown M_T/L
Linear rectangle	199	100	200	1.005	199	100	800	4.020
Quad. rectangle (Serendipity)	149	25	200	1.342	149	25	450	3.020
Quad. rectangle (Lagrange)	199	25	200	1.005	199	25	450	2.261
Linear triangle	199	200	400	2.010	199	200	1600	8.040
Quad. triangle	199	50	400	2.010	199	50	700	3.518

TABLE 8. DEGREE OF DEFINITENESS FOR MODERATE MESH

Element/ shape function combination	Reduced integration				Exact integration			
	Number of unknowns L	Number of elements e	No. of function eval. points M_T	Function eval. per unknown M_T/L	Number of unknowns L	Number of elements e	No. of function eval. points M_T	Function eval. per unknown M_T/L
Linear rectangle	399	200	400	1.003	399	200	1600	4.010
Quad. rectangle (Serendipity)	299	50	400	1.338	299	50	900	3.010
Quad. rectangle (Lagrange)	399	50	400	1.003	399	50	900	2.256
Linear triangle	399	400	800	2.005	399	400	3200	8.020
Quad. triangle	399	100	800	2.005	399	100	1400	3.509

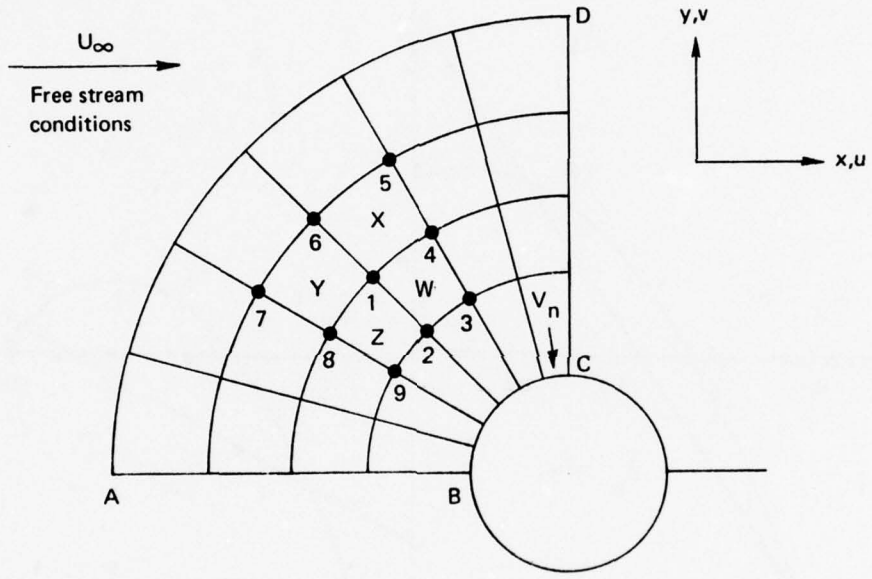

Figure 1. Flow field geometry

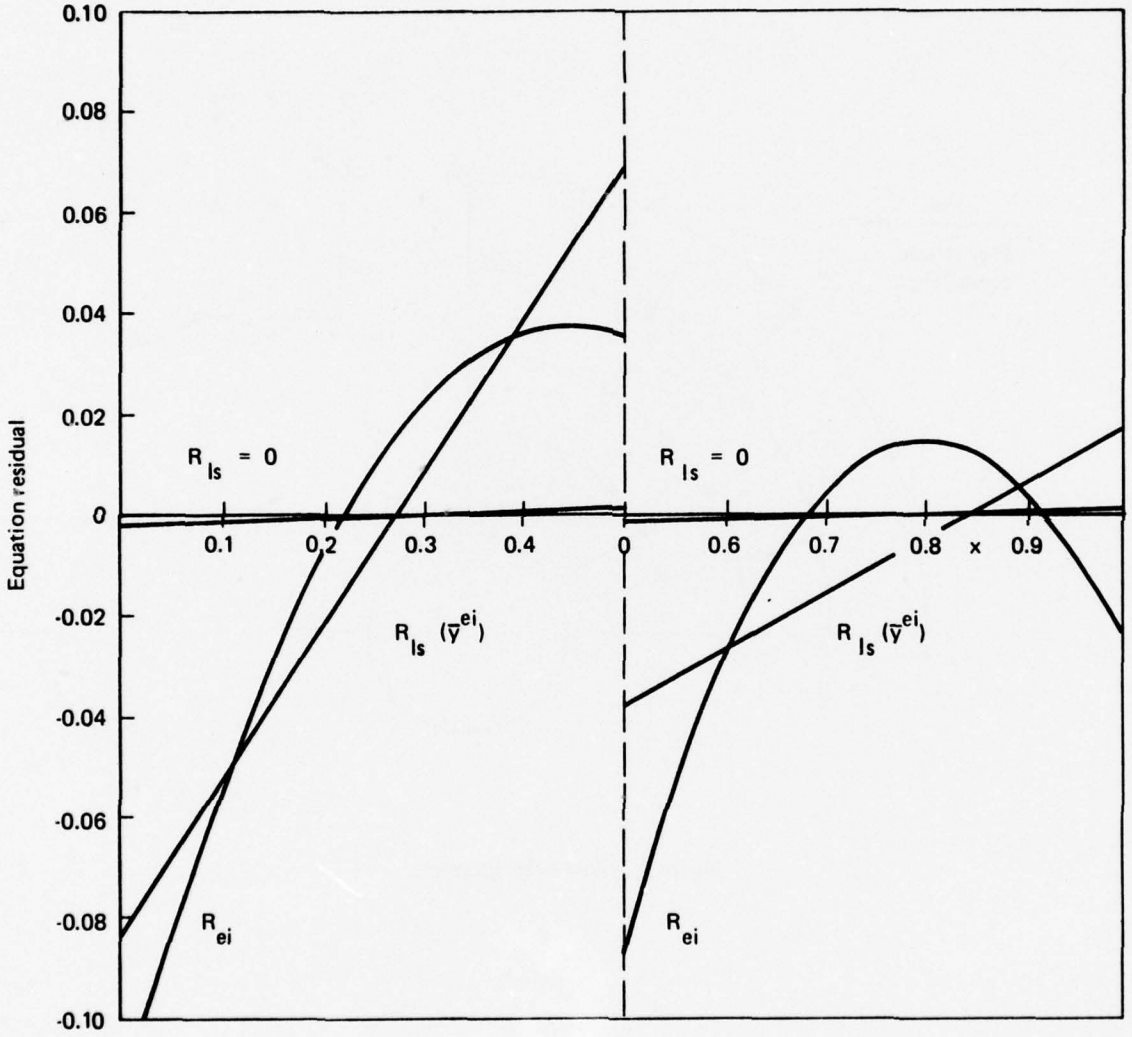

Figure 2. Variation of equation residuals for $\frac{dy}{dx} - y = 0$

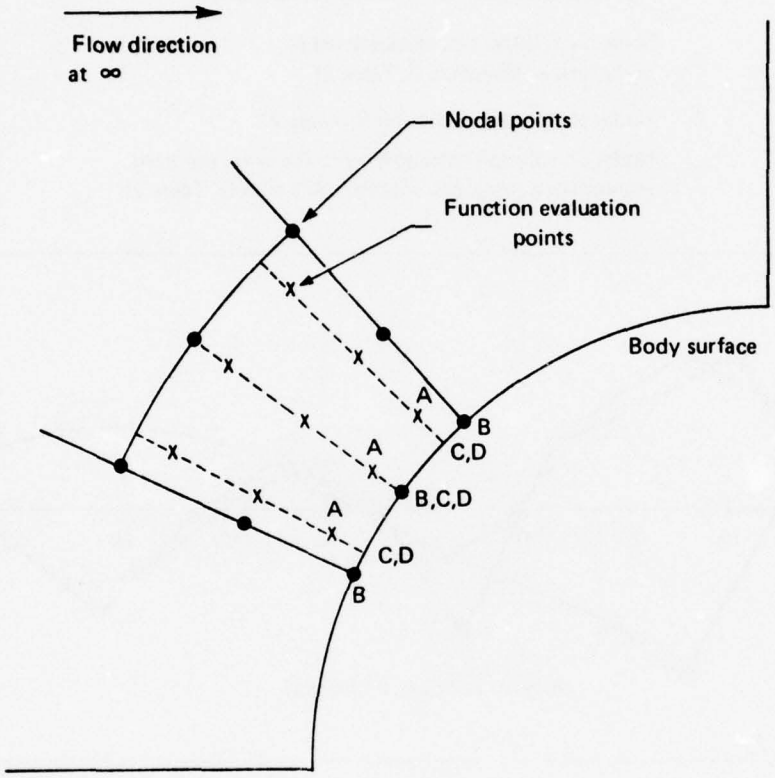

Figure 3. Alternative sampling points

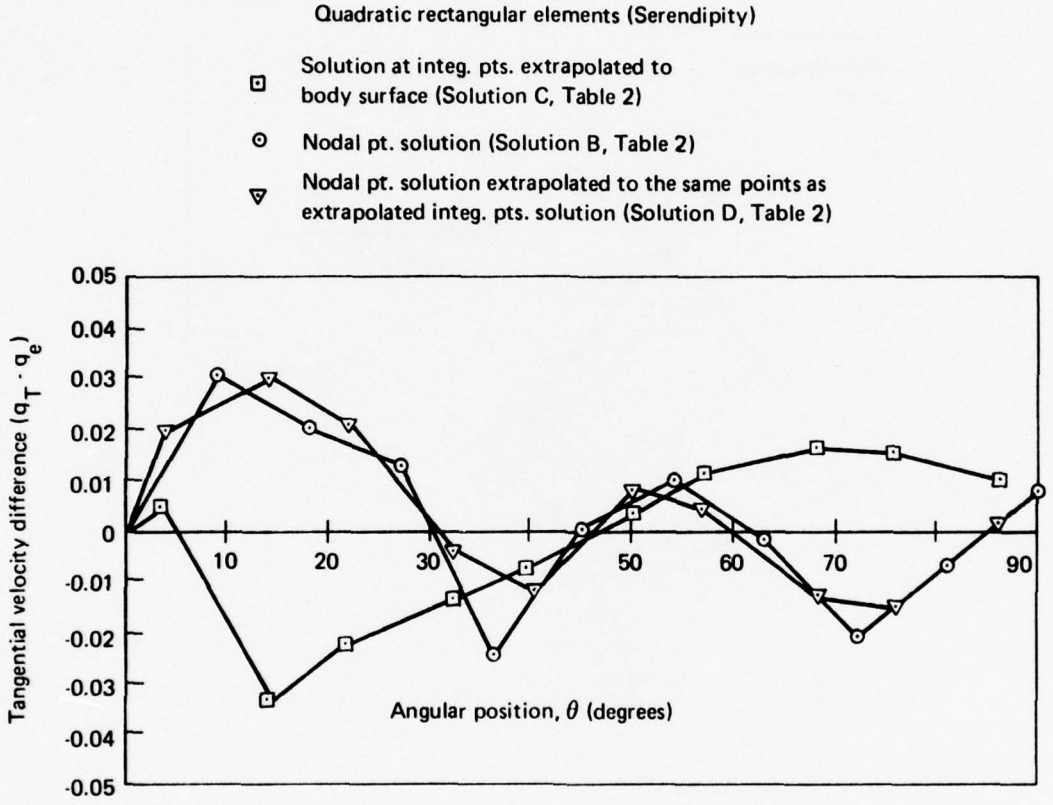

Figure 4. Variation of tangential velocity differences with angular position : 4 point integration formula

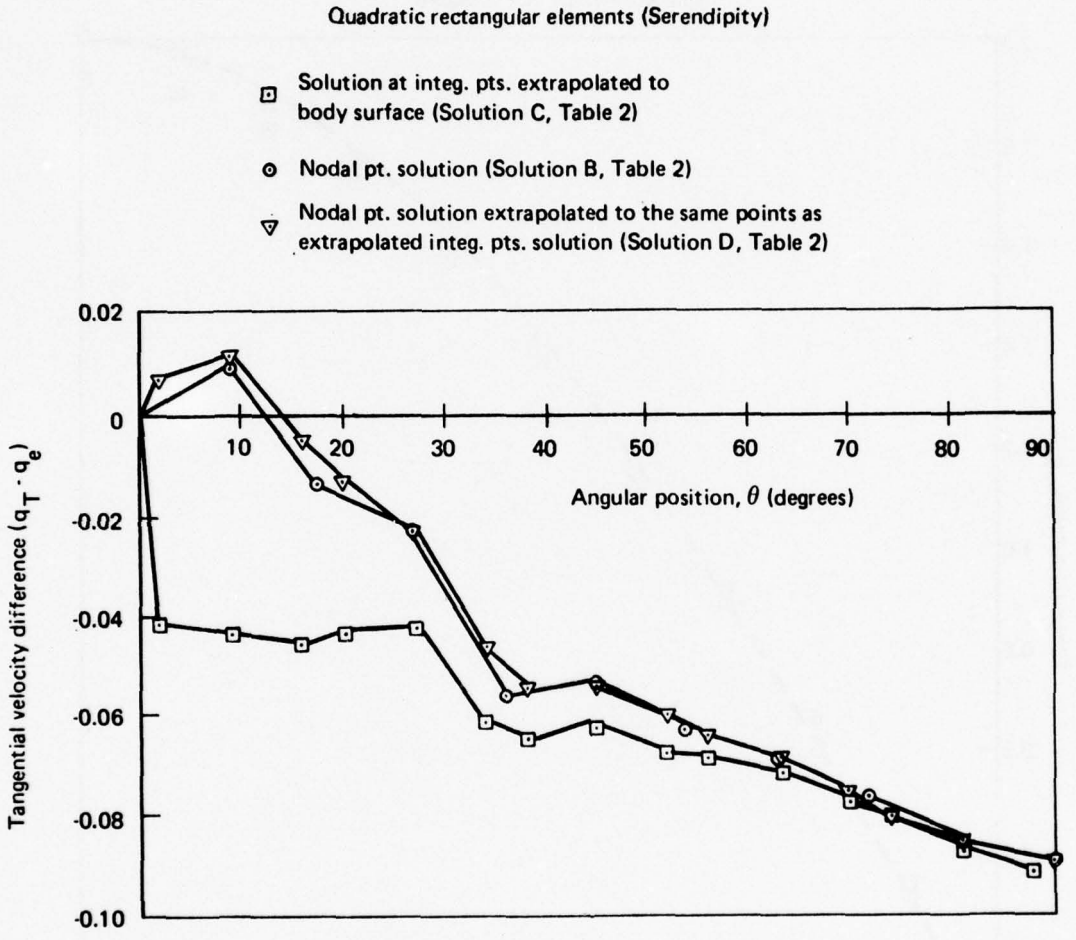

Figure 5. Variation of tangential velocity differences with angular position : 9 point integration formula

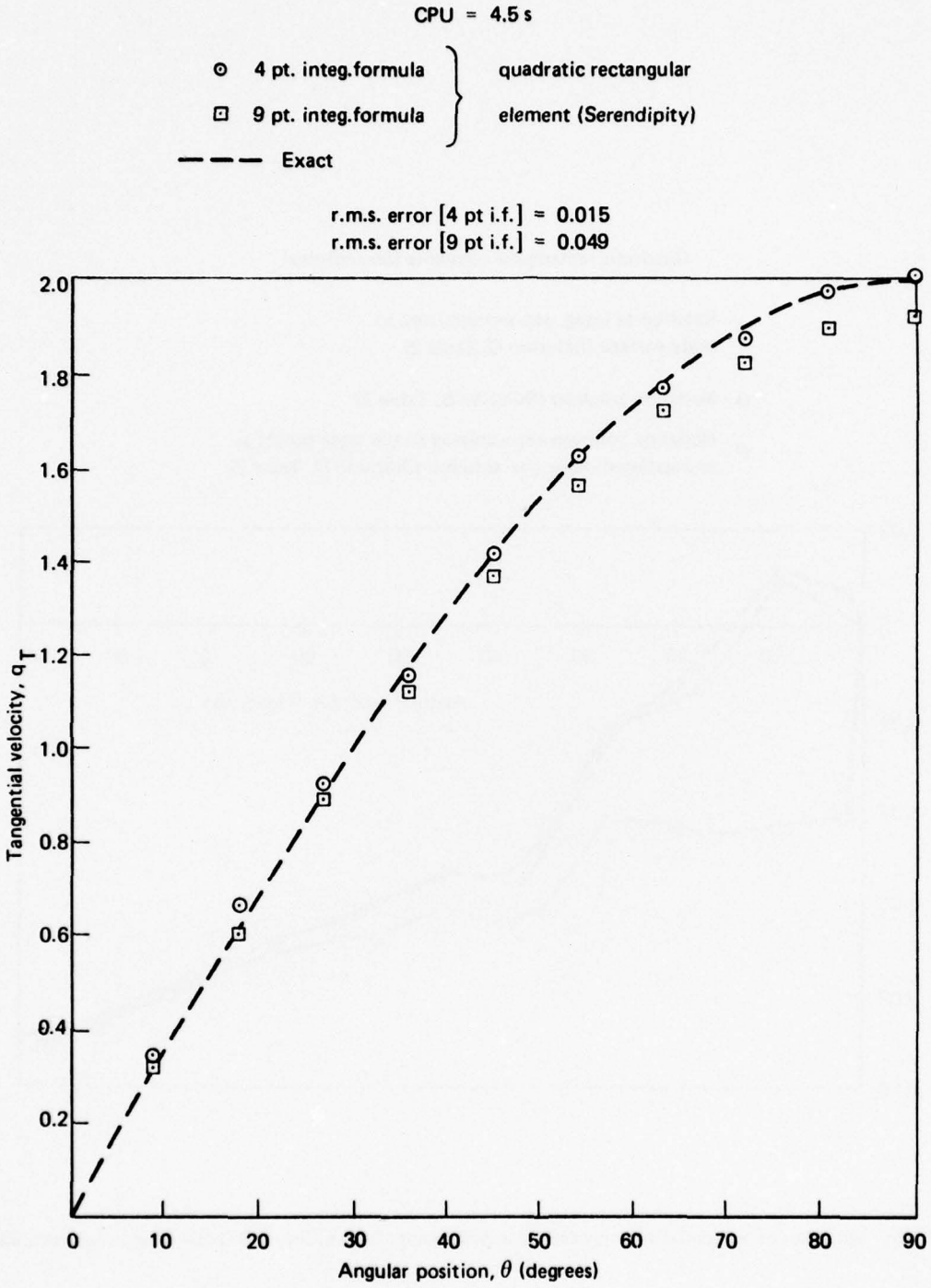

Figure 6. Comparison of accuracy of reduced integration and exact integration on a coarse grid

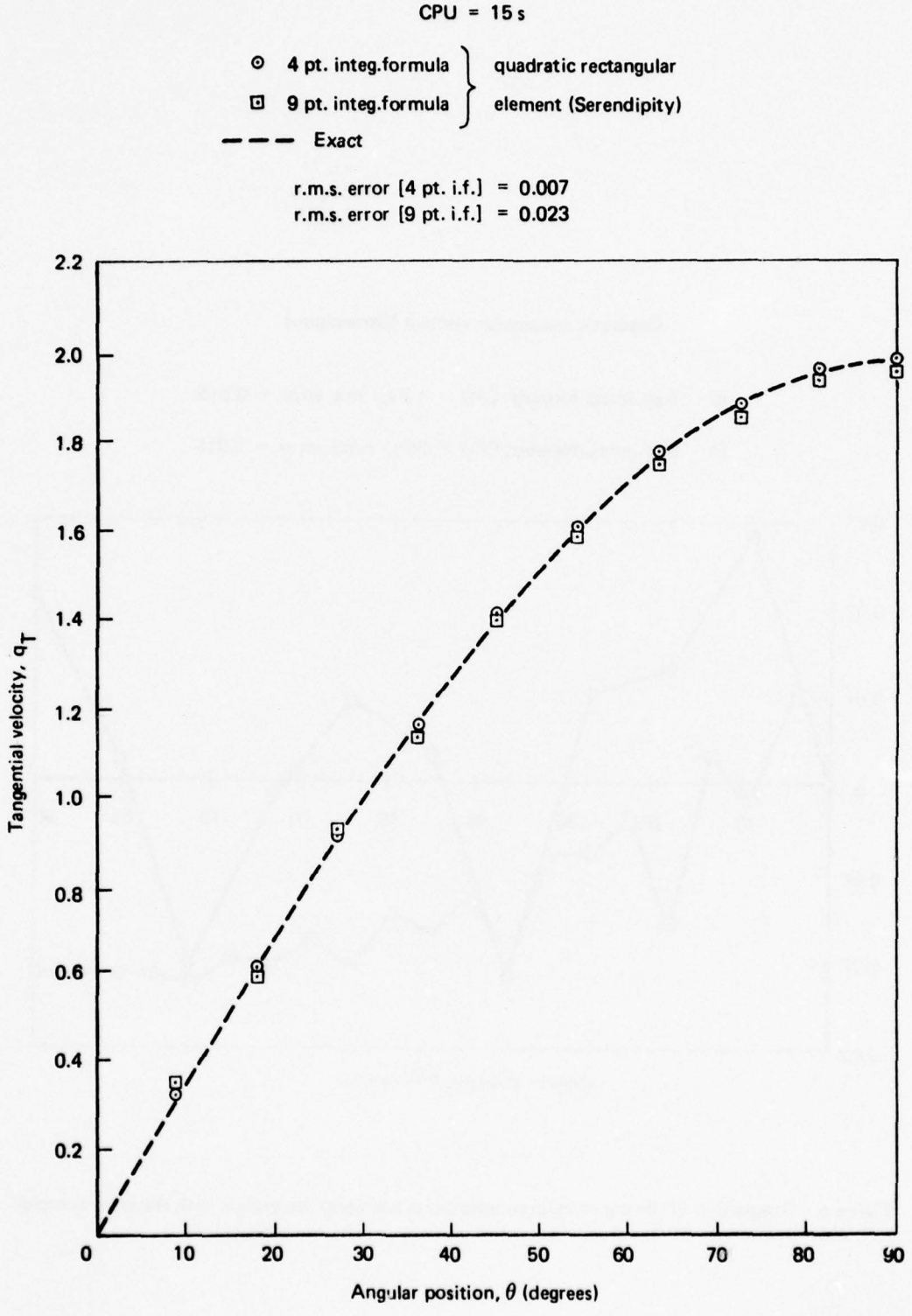

Figure 7. Comparison of accuracy of reduced integration and exact integration on a moderate grid

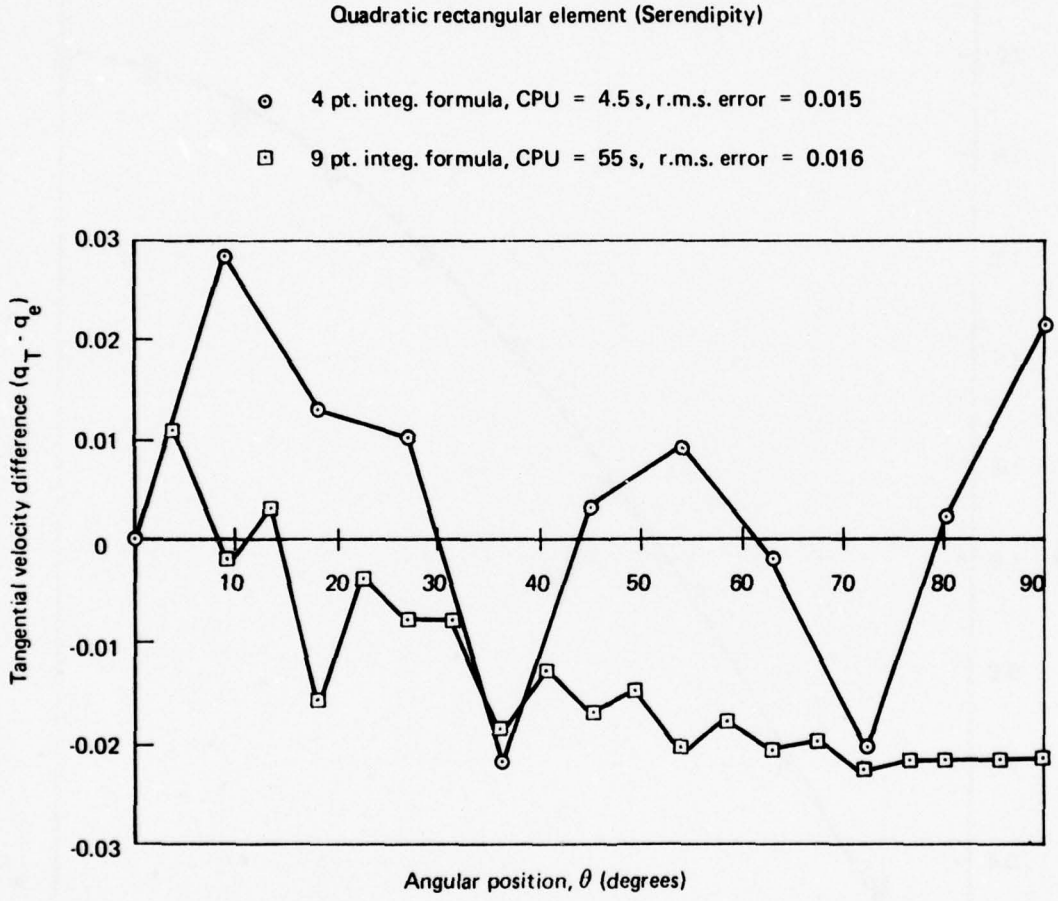

Figure 8. Comparison of the use of reduced integration and exact integration with the same accuracy

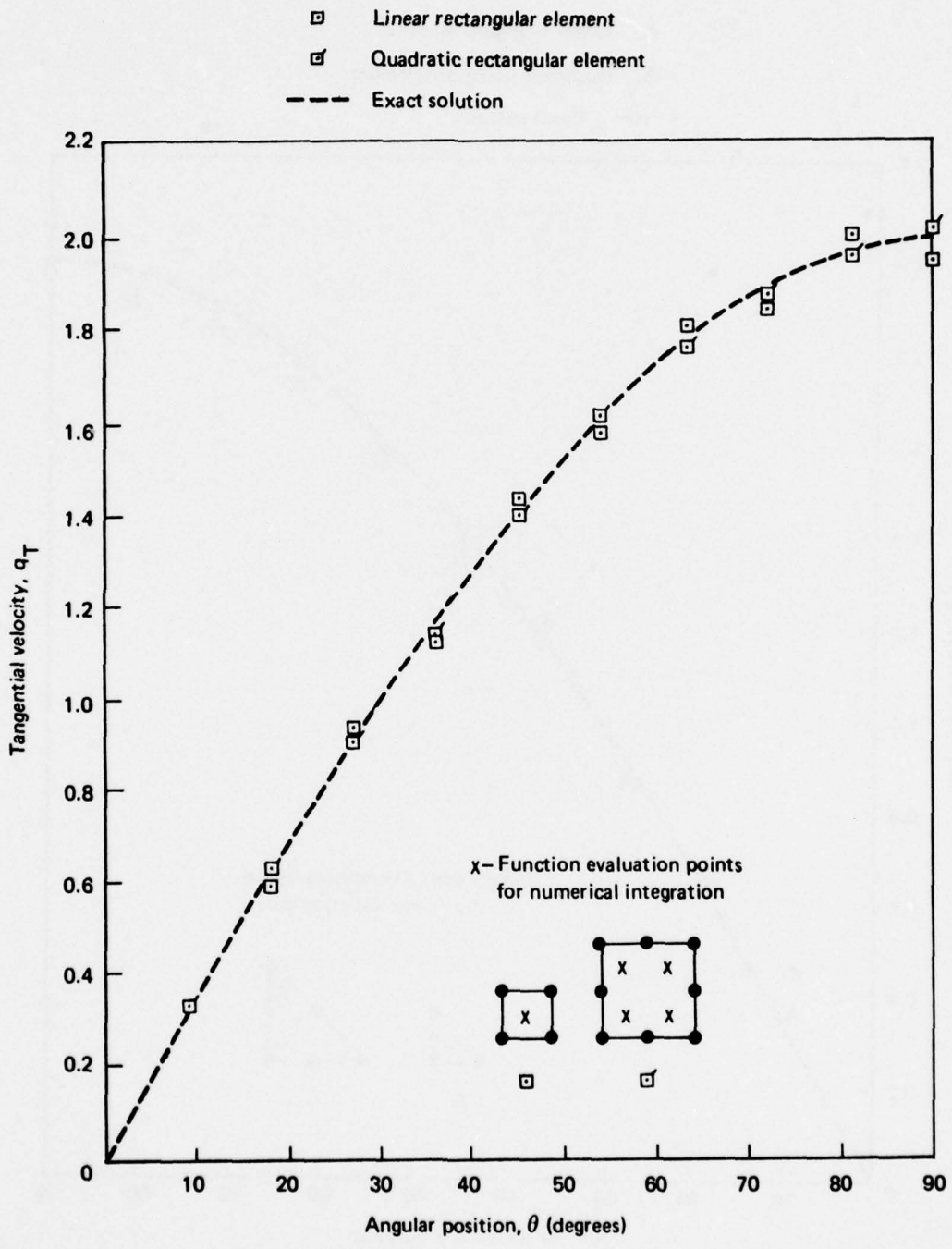

Figure 9. Comparison of linear and quadratic shape functions - rectangular elements - coarse grid - reduced integration

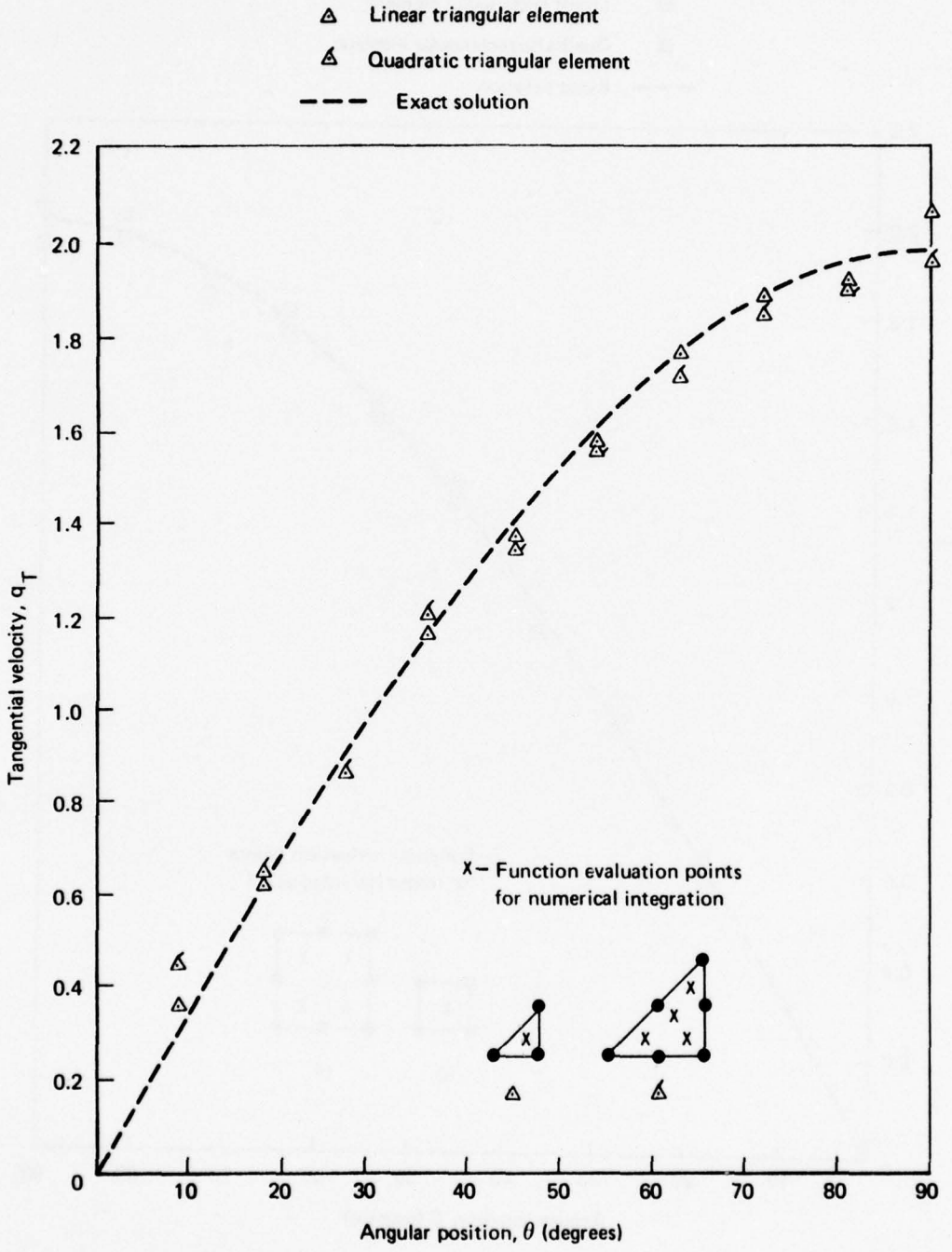

Figure 10. Comparison of linear and quadratic shape functions - triangular elements - coarse grid- reduced integration

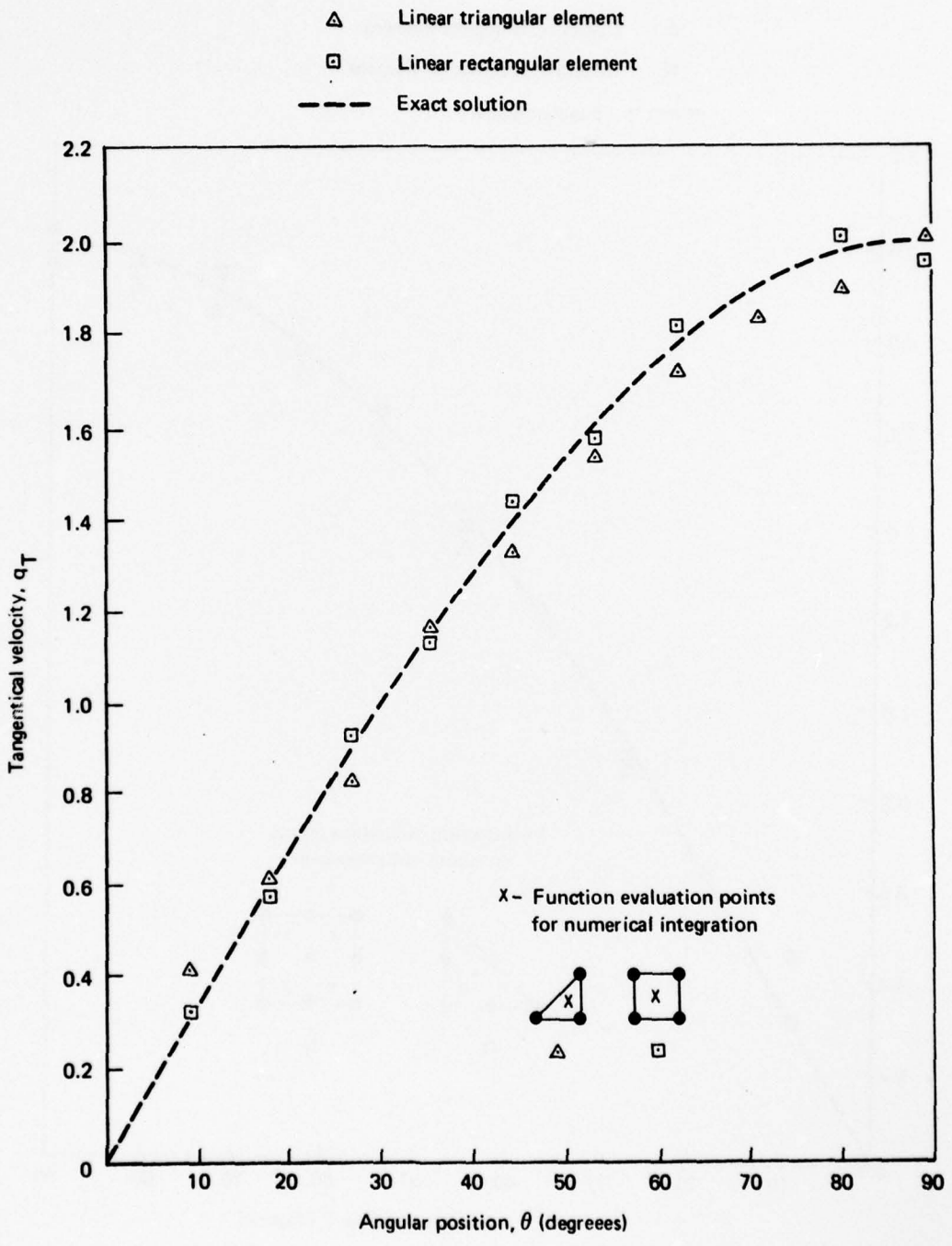

Figure 11. Comparison of triangular and rectangular elements - linear shape function - coarse grid - reduced integration

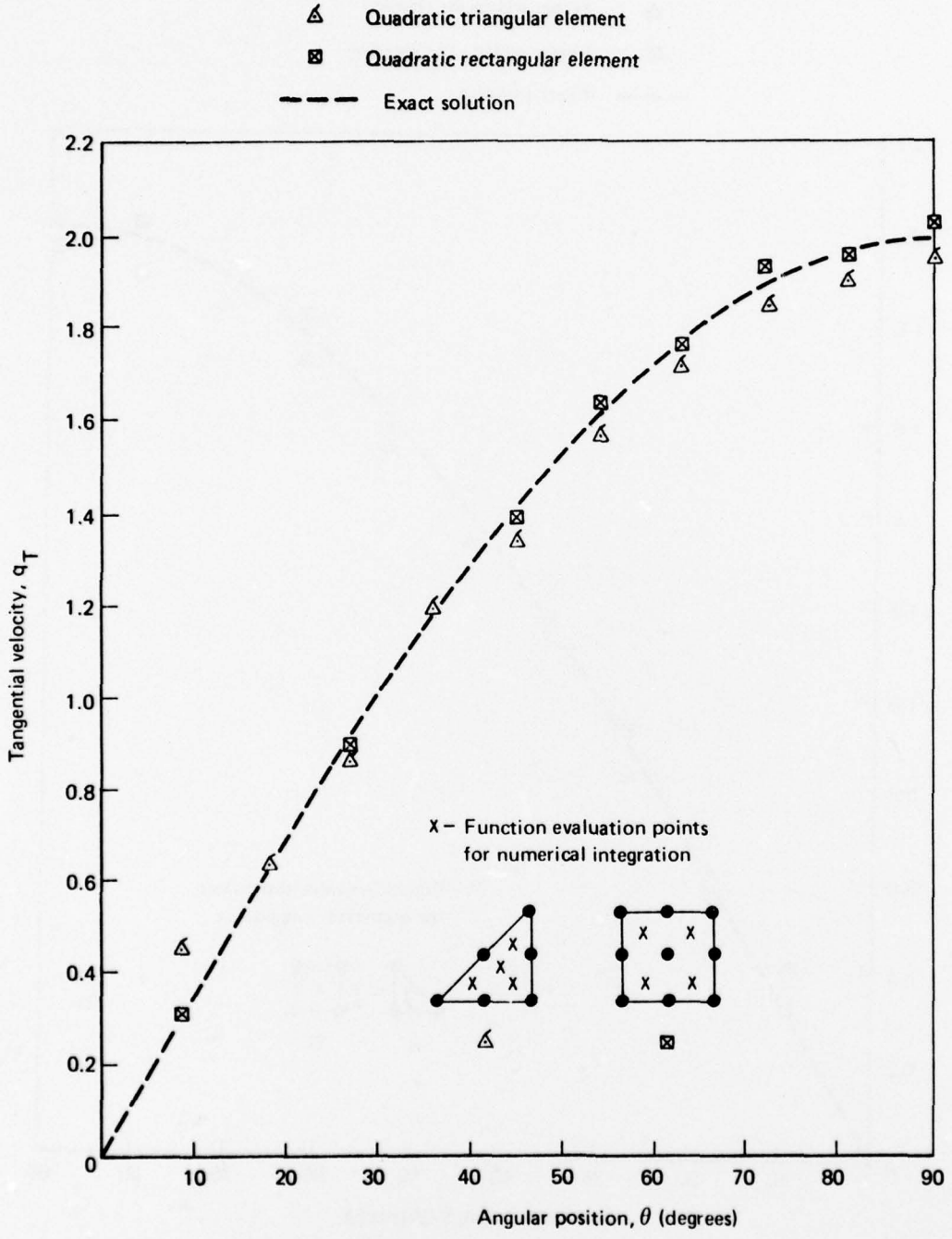

Figure 12. Comparison of triangular and rectangular elements - quadratic shape function - coarse grid - reduced integration

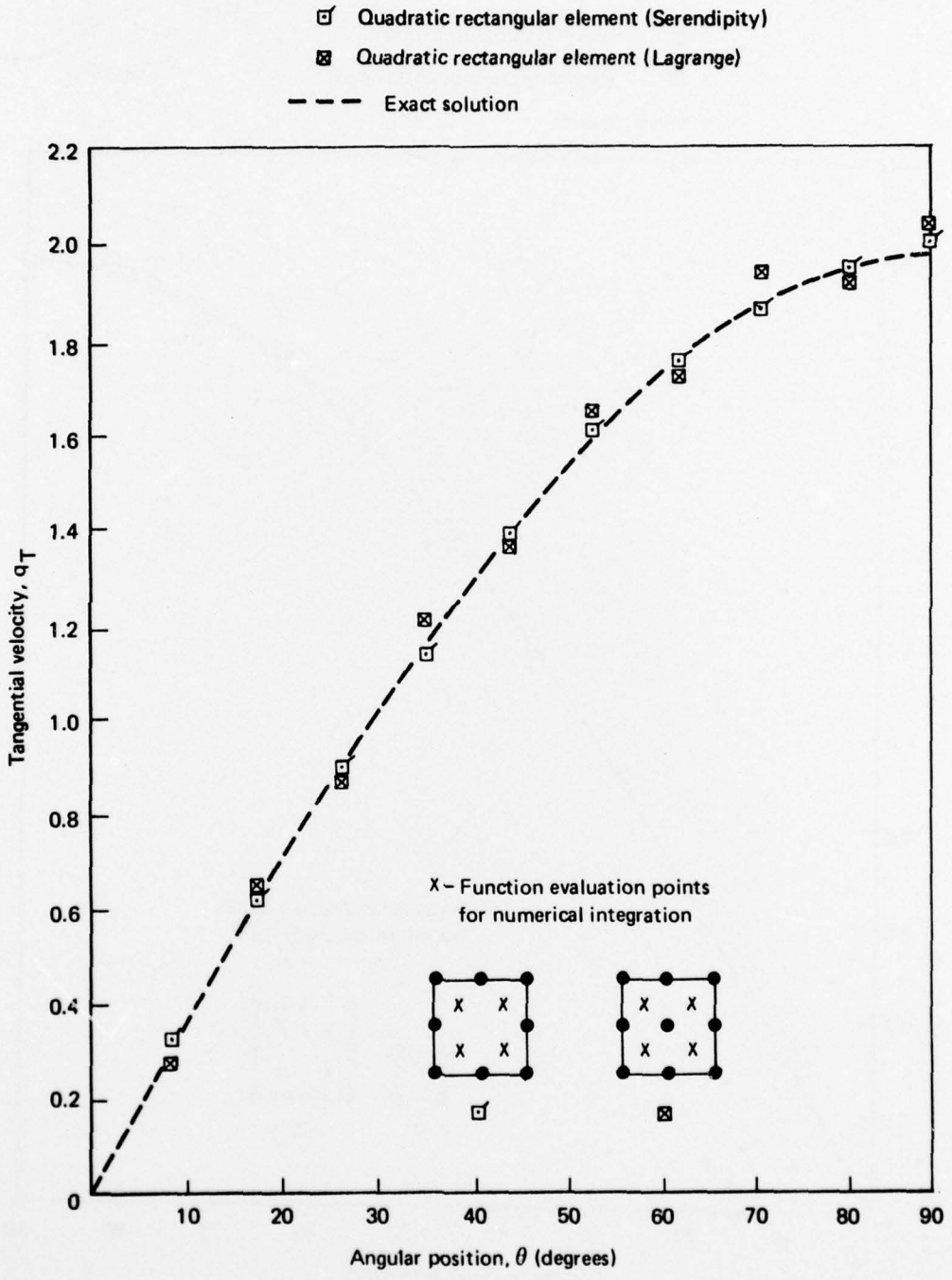

Figure 13. Comparison of Lagrange and Serendipity quadratic elements - coarse grid - reduced integration

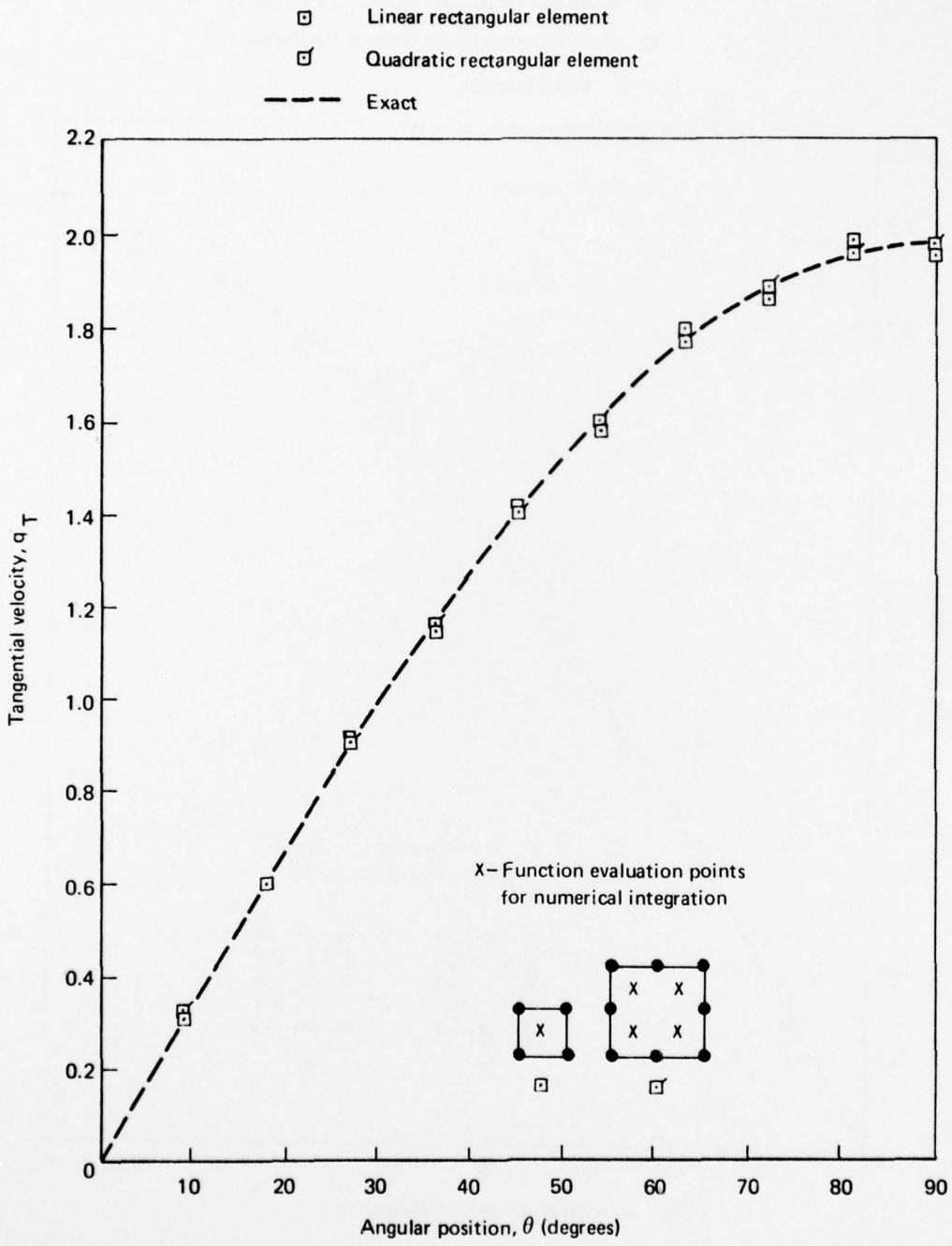

Figure 14. Comparison of linear and quadratic shape functions - rectangular elements - moderate grid - reduced integration

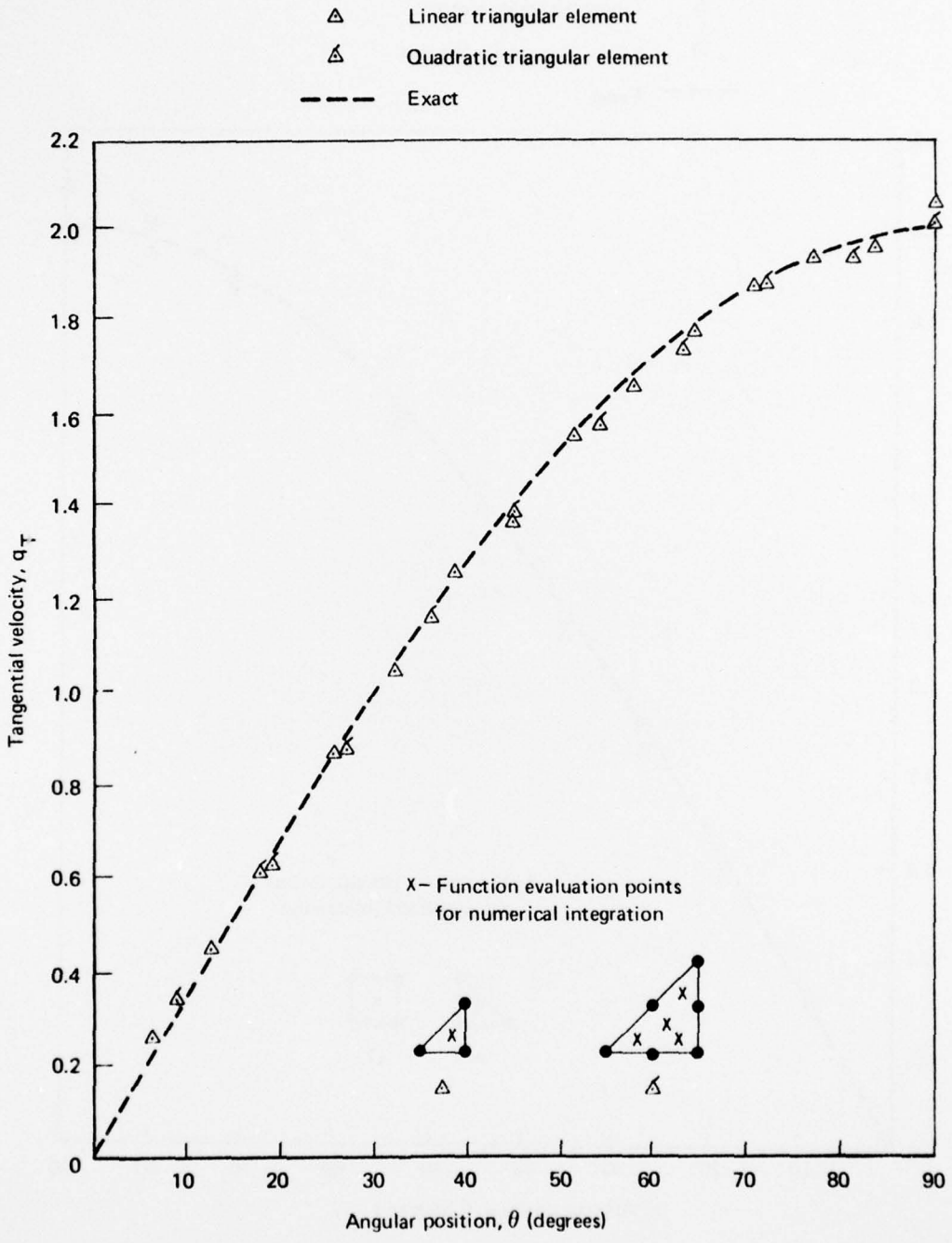

Figure 15. Comparison of linear and quadratic shape functions - triangular elements - moderate grid - reduced integration

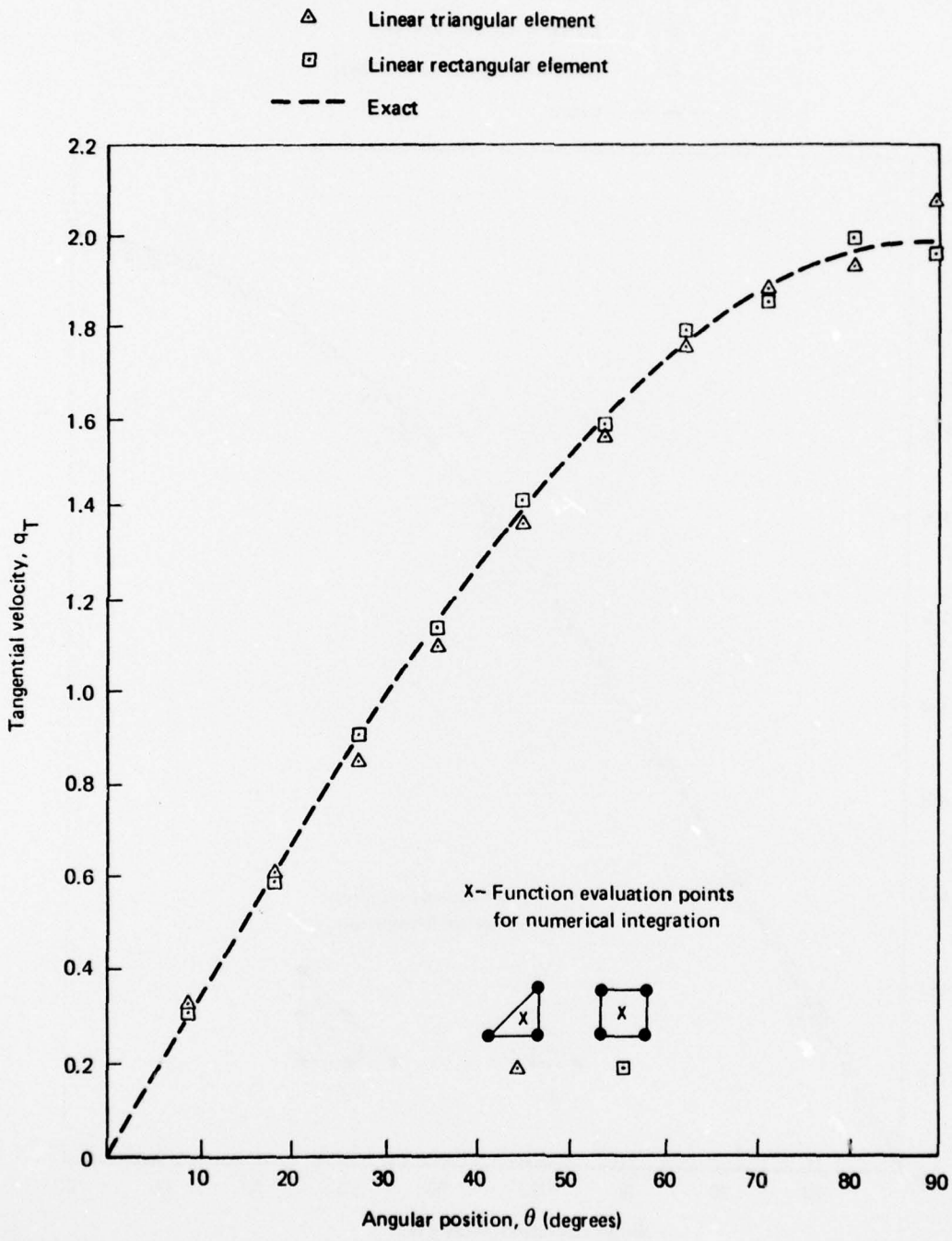

Figure 16. Comparison of triangular and rectangular elements - linear shape function - moderate grid - reduced integration

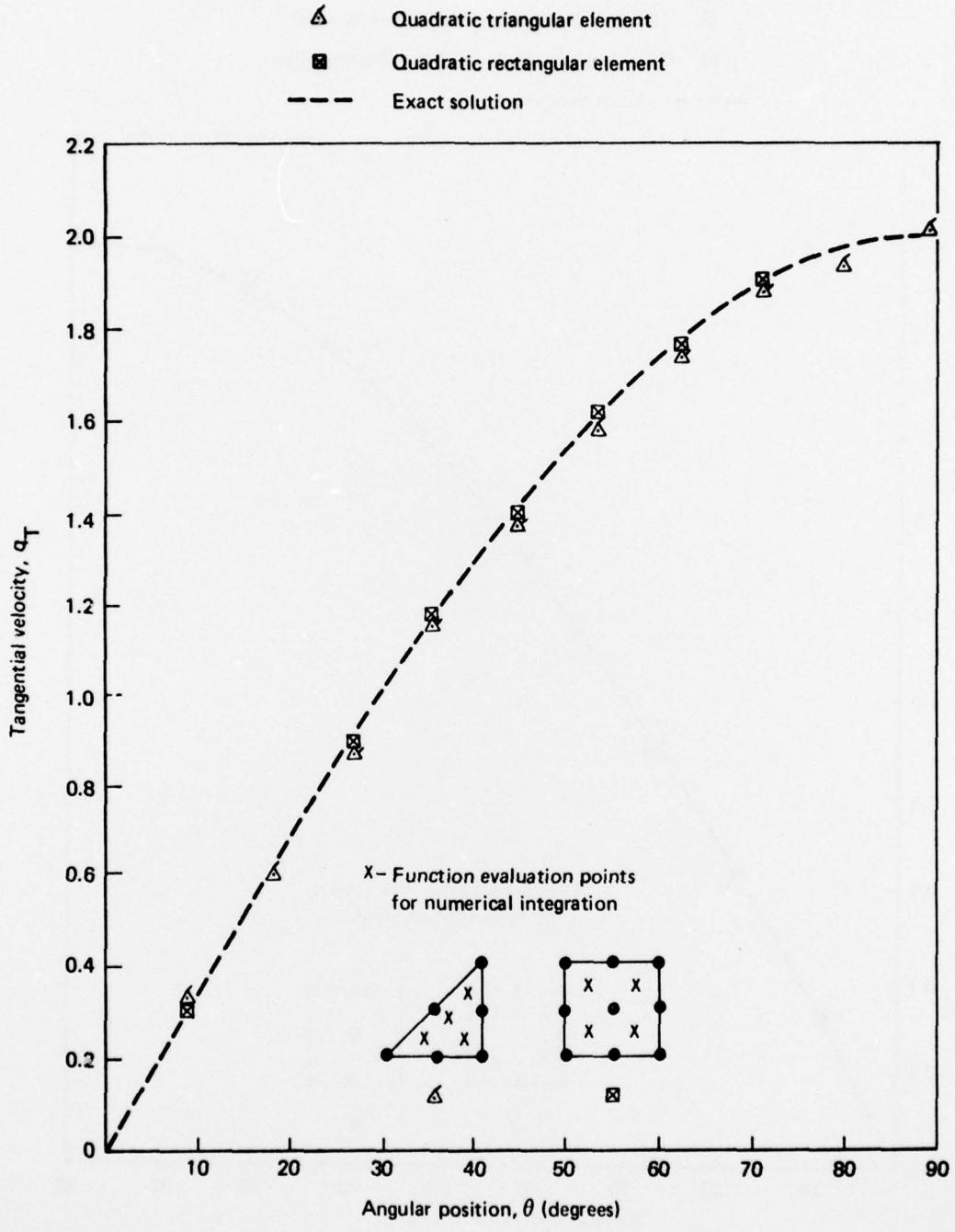

Figure 17. Comparison of triangular and rectangular elements - quadratic shape function - moderate grid - reduced integration

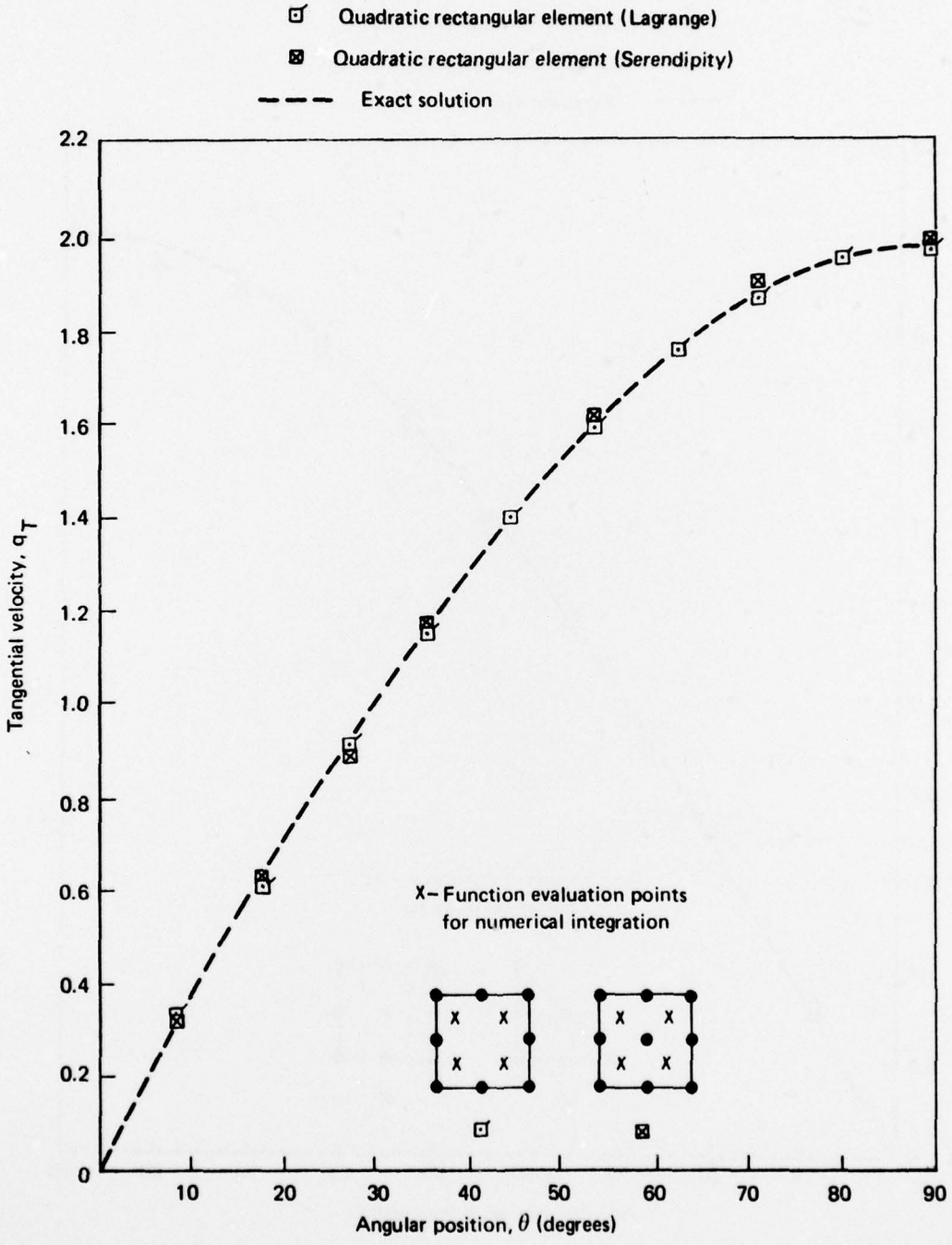

Figure 18. Comparison of Lagrange and Serendipity quadratic elements - moderate grid - reduced integration

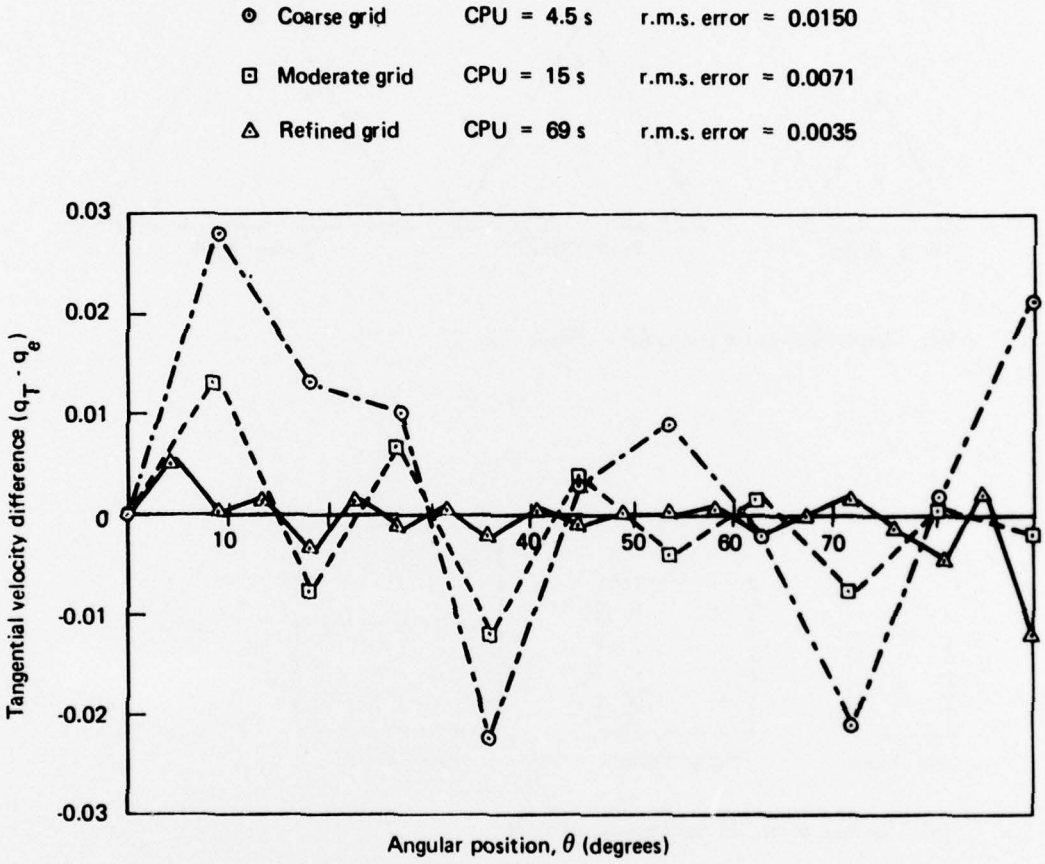

All solutions obtained with quadratic (Serendipity) rectangular elements and reduced integration

Figure 19. Effect of grid refinement

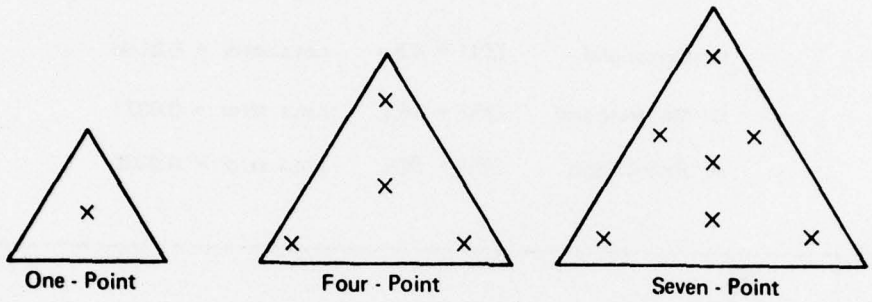

(a) Sample points for triangular elements

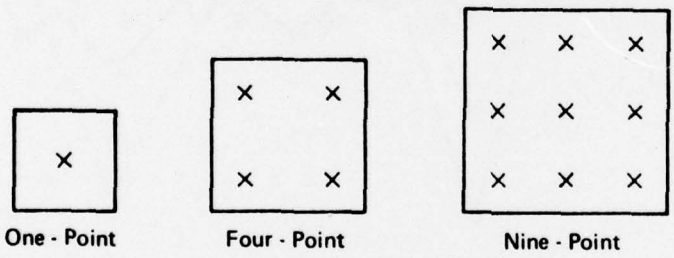

(b) Sample points for rectangular elements

Figure 20. Sample points for numerical integration formulae

DISTRIBUTION

EXTERNAL	Copy No.
In United Kingdom	
Defence Scientific and Technical Representative, London	1
Defence Research and Development Representative, London	2
Ministry of Defence, Defence Research Information Centre	3
Royal Aircraft Establishment	
Aero Department	4 - 5
Space Department	6
Weapons Department	7 - 8
Bedford	9
Library	10
R.A.R.D.E.	11
T.T.C.P., U.K. National Leader Panel W-2	12 - 15
Aeronautical Research Council	16 - 17
Aircraft Research Association (Bedford)	18
C.A.A.R.C. Secretary	19
National Lending Library of Science and Technology	20
Royal Aeronautical Society, Library	21
Cranfield Institute of Technology, Library	22
Imperial College, Department of Aeronautical Engineering Library	23
Queen Mary College, Department of Aeronautical Engineering	24
University of Bristol, Department of Aeronautical Engineering	25
University of Manchester, Department of Mechanics of Fluids	26
University of Southampton, Department of Aeronautics and Astronautics	27
University College of Swansea, Department of Civil Engineering (Professor O.C. Zienkiewicz)	28
Brunel University, Department of Mathematics (Professor J.R. Whiteman)	29
In United States	
Counsellor, Defence Science, Washington	30
Defence Research and Development Attache, Washington	31
Department of Defense, Defense Documentation Center	32 - 43
Air Force Armament Testing Laboratory	44
Ballistic Research Laboratories	45
Edgewood Arsenal	46
Eglin Air Force Base	47
N.A.S.A.	48 - 51
Naval Surface Weapons Center	
Dahlgren	52
White Oak	53

	Copy No.
Naval Weapons Center	54
Naval Ship Research and Development Center	55
Naval Weapons Laboratory	56
Picatinny Arsenal	57
Redstone Arsenal	58
T.T.C.P. U.S. National Leader Panel W-2	59 - 62
Wright-Patterson Air Force Base, Library	63
American Institute of Aeronautics and Astronautics, Library	64
Pacific Technical Information Services, Northrop Institute of Technology	65
Applied Mechanics Reviews	66
Arnold Engineering Development Center	67
A.R.O. Inc.	68
The Boeing Company, Library	69
Lockheed Aircraft Corporation, Library	70
McDonnell-Douglas Corporation, Library	71
Sandia Corporation, Library	72
Bell Aerospace Division of Textron (Dr. A.J. Baker)	73
Douglas Aircraft Company, Library Long Beach	74
University of Washington, Department of Chem. Eng. (Professor B.A. Finlayson)	75
University of California, Berkeley, Department of Mech. Eng. (Professor M. Holt)	76
University of California, Berkeley, Department of Mech. Eng., Library	77
Mass. Inst. of Technology, Aeronautics Department, Library	78
Polytechnic Inst. of Brooklyn, Department of Aero. Eng. (Professor G. Moretti)	79
New York University, Courant Inst. of Math. Sci., Library	80
The University of Texas, Austin (Professor J.T. Oden)	81
Princeton University, Department of Aeronautics, Library	82
Stanford University, Department of Aeronautics, Library	83
The Aerospace Corp., Fluid Mechanics Department (Dr. T. Taylor)	84
University of California, Berkeley, Department of Civil Eng. (Professor R.L. Taylor)	85
T.R.W. Systems, Library	86

	Copy No.
United Aircraft Research Labs., Library	87
University of Maryland, Institute of Fluid Dynamics and Applied Math., Library	88
In Canada	
Defence Research Establishment, Valcartier	89
Ministry of Defence, Defence Science Information Service	90
N.A.E., Ottawa	91
T.T.C.P., Canadian National Leader Panel W-2	92 - 95
University of Toronto, Institute of Aerospace Studies	96
McGill University, Library, Montreal	97
University of Calgary, Department of Mechanical Engineering (Professor D.H. Norrie)	98
In Europe	
A.G.A.R.D., Brussels	99 - 104
University of Paris South, Orsay, Department of Mathematics (Professor R. Temam)	105
National Aerospace Lab., Holland (Dr. J. van der Vooren)	106
In India	
Aeronautical Development Establishment, Bengalore	107
Indian Institute of Science, Bangalore (Department of Aero Engineering)	108
Indian Institute of Technology, Madras (Department of Aero Engineering)	109
Hindustan Aeronautics Ltd., Bangalore	110
National Aeronautical Lab., Bangalore	111
Space Science and Technology Centre, Trivandrum	112
In New Zealand	
Ministry of Defence	113
In Australia	
Department of Defence, Canberra	
Defence Library, Campbell Park	114
Air Force Scientific Adviser	115 - 116
Army Scientific Adviser	117 - 118
Navy Scientific Adviser	119 - 120
Defence Science and Technology	
Chief Defence Scientist	121
Executive Controller, Australian Defence Scientific Service	122
Controller, Programme Planning and Policy	123

	Copy No.
Superintendent, Defence Science Administration	124
Superintendent, Central Studies Establishment	125
Assistant Secretary, Defence and Information Services (for microfilming)	126
B.D.R.S.S., Canberra	127 - 128
Superintendent, Aeronautical Research Laboratories, Mech. Eng. Division	129
Director, Joint Intelligence Organisation (DDSTI)	130
Superintendent, Aeronautical Research Laboratories, Aerodynamics Division	131
Superintendent, Aeronautical Research Laboratories, Mech. Eng. Division	132
Aeronautical Research Laboratories, Library	133
Materials Research Laboratory, Library	134
Department of Industry and Commerce, Melbourne	
Government Aircraft Factories	135
R.A.A.F., Academy, Point Cook	136
C.A.C.	137
Institute of Engineers, Australia	138
Australian National University, Library	139
Australian National University, Computing Centre	
(Dr. R.S. Anderssen)	140
C.S.I.R.O., Chief of Division of Mechanical Engineering	141
C.S.I.R.O., Chief of Division of Meteorological Physics	142
Flinders University, Library	143
Monash University, Library	144
University of Adelaide, Library	145
University of Adelaide, Department of Applied Mathematics	
(Dr. B.J. Noye)	146
University of Adelaide, Department of Civil Eng.	
(Professor Y.K. Cheung)	147
University of Adelaide, Department of Civil Eng.	
(Dr. S.G. Hutton)	148
University of Melbourne, Library	149
University of Newcastle, Library	150
University of New South Wales, Library	151
University of New South Wales,Department of Mechanical Engineering	
(Professor G. de Vahl Davis)	152
University of New South Wales, Dean of Engineering	
(Professor P.T. Fink)	153
University of Queensland, Department of Mechanical Engineering, Library	154

	Copy No.
University of Sydney, Library	155
University of Sydney, Department of Aero. Eng. (Dr. G.P. Steven)	156
University of Sydney, Department of Mechanical Engineering (Professor R.I. Tanner)	157
University of Tasmania, Library	158
University of Western Australia, Library	159
Caulfield Institute of Technology, Department of Mathematics (Dr. A.K. Easton)	160
INTERNAL	
Director	161
Chief Superintendent, Weapons Research and Development Wing	162
Superintendent, Aerospace Division	163
Head, Ballistics Composite	164
Principal Officer, Dynamics Group	165
Principal Officer, Aerodynamics Research Group	166
Principal Officer, Ballistic Studies Group	167
Principal Officer, Field Experiments Group	168
Principal Officer, Flight Research Group	169
Author	170
W.R.E. Library	171 - 172
A.D. Library	173 - 174
Spares	175 - 197